JOURNAL OF PETROLOGY | VOLUME 0 | NUMBER 0 | PAGES 1–27 | 2012 | doi:10.1093/petrology/egs019

Journal of Petrology Advance Access published April 6, 2012

Laurentian Provenance of Archean Mantle Fragments in the Proterozoic Baltic Crust of the Norwegian Caledonides

E. E. BEYER[1,2]*, H. K. BRUECKNER[1,3,4], W. L. GRIFFIN[1] AND S. Y. O'REILLY[1]

[1]ARC NATIONAL KEY CENTRE FOR GEOCHEMICAL EVOLUTION AND METALLOGENY OF CONTINENTS, MACQUARIE UNIVERSITY, NSW 2109, AUSTRALIA

[2]NORTHERN TERRITORY GEOLOGICAL SURVEY, P.O. BOX 8760, ALICE SPRINGS, NT 0871, AUSTRALIA

[3]QUEENS COLLEGE AND THE GRADUATE CENTER OF THE CITY UNIVERSITY OF NEW YORK, FLUSHING, NY 11367, USA

[4]LAMONT–DOHERTY EARTH OBSERVATORY OF COLUMBIA UNIVERSITY, PALISADES, NY 10964, USA

RECEIVED DECEMBER 20, 2009; ACCEPTED FEBRUARY 15, 2012

The Proterozoic gneisses of the Western Gneiss Region (WGR) of western Norway experienced HP–UHP metamorphism during the 435–390 Ma Caledonian (Scandian) orogeny, and locally enclose numerous large bodies of Archean peridotite. Competing models for the emplacement of these peridotites into the gneisses involve either (1) upthrusting of subcontinental mantle into overlying gneisses or (2) 'sinking emplacement' of peridotites from the Laurentian mantle wedge into the upper surface of the subducting Baltica plate. The first model implies the existence of Archean lower crust below the outcropping gneisses. To evaluate these models we have carried out a regional survey of the U–Pb age, Hf isotope composition and trace-element compositions of detrital zircon grains collected from drainages in the northern half of the WGR. The zircon data indicate that the gneisses that make up the crust of the WGR were originally generated during the 1·7–1·5 Ga Gothian orogeny. The Hf isotope signatures of these zircons indicate a juvenile (i.e. mantle) origin; there is no evidence, from either inherited zircons or the Hf isotope data, that Archean crustal materials were involved in the genesis of these gneisses. The Sveconorwegian orogeny (1·3 to <1·0 Ga) that overprinted the Gothian gneisses involved both juvenile magmatic additions to the crust and remelting of the Gothian basement; these Sveconorwegian-age magmas also show no evidence of Archean contributions. A population of zircons collected from a drainage area containing large mantle-derived peridotite bodies includes anhedral to rounded grains with distinctive trace-element patterns consistent with derivation from depleted rocks; these are inferred to be derived from the peridotites and/or their enclosed eclogites and pyroxenites. These zircons give Archean Hf model ages, but $^{207}Pb/^{206}Pb$ ages ranging from Archean to Caledonian, suggesting that the younger ages reflect resetting during later thermal events. The Archean zircon ages are consistent with Archean Re–Os model ages previously obtained on the peridotites. In the absence of any evidence for Archean crust (and hence Archean mantle) beneath southern Baltica, we infer that the peridotite massifs represent fragments of the subcontinental lithosphere beneath Laurentia, and were introduced tectonically into the gneisses during the Caledonian subduction of Baltica beneath Laurentia.

KEY WORDS: *Western Gneiss Region; Baltica–Laurentia; Caledonian orogeny; peridotite zircons*

INTRODUCTION

Bodies of mantle-derived peridotite enclosed in the Proterozoic gneisses of the Western Gneiss Region (WGR) of western Norway have been shown to have an Archean origin, based on Re–Os dating of both whole-rock samples and their sulfides (Brueckner *et al.*, 2002; Beyer *et al.*, 2004). This discrepancy in ages between the peridotites

*Corresponding author. Present address: Northern Territory Geological Survey, P.O. Box 8760, Alice Springs, NT 0871, Australia. E-mail: Eloise.Beyer@nt.gov.au

and their host-rocks raises the question of how the peridotites were emplaced into the gneisses. If the peridotites were thrust up from an underlying mantle of Archean age, we might expect there would be Archean lower crust somewhere in the WGR, which has not yet been recognized. An alternative is that the peridotites represent fragments of the Laurentian lithospheric mantle, which is at least partially of Archean age (Thrane, 2002; Higgens *et al.*, 2004; Waldron *et al.*, 2008). These fragments could have been scraped off the base of the Laurentian mantle wedge by the gneisses as Baltica was thrust under Laurentia to produce the well-known Caledonian high-pressure–ultrahigh-pressure (HP–UHP) metamorphism within the WGR.

This problem has prompted a geochronological and isotopic study of detrital zircons derived from the WGR gneisses and associated rock types, to determine if there is any evidence of an Archean component to the crust in this part of the Baltic Shield. Although it is possible that Archean crust might have been present but was overprinted by later metamorphic events, it is unlikely that zircons within these rocks would have lost all evidence for this ancient origin. We have used GEMOC's *TerraneChron*® approach, which is based on the integrated *in situ* analysis of zircons (in this case detrital) for U–Pb age, Hf-isotope composition and trace-element patterns. This approach has proven valuable for studies of crustal evolution (e.g. Belousova *et al.*, 2009, 2010) and can be readily applied to give a broad picture of crustal evolution in tectonically complex areas such as western Norway.

REGIONAL SETTING

The Scandinavian Caledonides form a 1000 km long mountain system composed of nappe units (i.e. the lower, middle, upper and uppermost allochthons, Fig. 1) that were assembled into a single linear orogenic belt during the 435–390 Ma Scandian Orogeny, which accompanied the final closure of the Iapetus Ocean (Roberts & Gee, 1985; Stephens & Gee, 1989; Roberts, 2003; Brueckner & Van Roermund, 2004; Spengler *et al.*, 2009). During this terminating collision the nappes were thrust, or re-thrust, toward the east or SE (present coordinates) over the crystalline rocks of the Baltic Shield, consistent with a geometry in which the western continent (Laurentia) overthrust the eastern continent (Baltica; Cuthbert *et al.*, 1983; Harley & Carswell, 1995).

The WGR of western Norway lies beneath the nappes and is generally interpreted to have been part of the western edge of Baltica during this collision. The WGR contains hundreds of bodies of HP–UHP eclogites and other eclogite-facies rocks, including garnet peridotites. Most of the eclogites, as well as the host gneisses, give recrystallization ages of 425–390 Ma by Rb–Sr, Sm–Nd and Lu–Hf mineral isochrons (Brueckner, 1972, 1979; Griffin & Brueckner, 1980, 1985; Mearns & Lappin, 1982; Mørk & Mearns, 1986; Jamtveit *et al.*, 1991; Carswell *et al.*, 2003*a*; Kylander-Clark *et al.*, 2007; Peterman *et al.*, 2009), by ^{40}Ar–^{39}Ar (Root *et al.*, 2004, 2005; Walsh & Hacker, 2004; Walsh *et al.*, 2007) and by U–Pb in zircon and rutile (Gebauer *et al.*, 1985; Carswell *et al.*, 2003*b*; Krogh *et al.*, 2003; Root *et al.*, 2004; Kylander-Clark *et al.*, 2008). All of these data indicate that the HP–UHP metamorphism occurred during the Scandian Orogeny. The model that best explains the HP–UHP conditions and an apparent SE to NW increase in metamorphic grade (Fig. 1; Krogh, 1977; Cuthbert *et al.*, 2000; Root *et al.*, 2005) is that the WGR was subducted deeply into the mantle beneath Laurentia during collision, with the depth of subduction increasing towards the NW (Andersen *et al.*, 1991, 2001; Brueckner; 1998; Brueckner & Van Roermund, 2004; Hacker *et al.*, 2010).

The metamorphic rocks that make up the WGR and host the eclogites are mostly orthogneiss and paragneiss. Age determinations by Rb–Sr whole-rock methods (Brueckner, 1972) and U–Pb in zircon (Tucker *et al.*, 1987, 1990, 1992; Austrheim *et al.*, 2003; Skår & Pedersen, 2003; Root *et al.*, 2004, 2005; Young *et al.*, 2007) suggest that the bulk of the orthogneiss was generated by magmatism (±metamorphism?) during two major Proterozoic tectonic cycles; the Gothian (1·7–1·5 Ga) and Sveconorwegian (1·2–0·9 Ga); groups of U–Pb zircon ages also appear at *c.* 1455 and *c.* 1250 Ma. A single zircon from a metapelite gave an age of *c.* 2·1 Ga (Walsh *et al.*, 2007), making it the oldest zircon that we know of in the WGR.

Locally, the WGR contains strips of paragneisses, metasedimentary rocks (quartzites, marbles, aluminous schists) and mafic meta-igneous rocks (anorthosites, amphibolites, hornblende schists) that can be traced for hundreds of meters to several tens of kilometers. The origins of these rocks are debated, but there appears to be a growing consensus that many of these units are fragments of the nappes described above, which were accreted onto Baltica early in the Caledonian orogenic cycle (Brueckner & Van Roermund, 2004; Brueckner, 2006; Walsh *et al.*, 2007) and then re-deformed and re-metamorphosed ('Caledonized') during the final Scandian subduction. Thus far, with the single 2·1 Ga exception noted above, none of the country rocks from the WGR, or from the adjacent Precambrian shield of southern Norway or SW Sweden, have yielded dates earlier than *c.* 1·85 Ga. It appears that all rocks from the southwestern corner of the Baltic shield were generated from the mid-Proterozoic to the mid-Paleozoic.

Minor but important constituents of the WGR are hundreds of mantle-derived ('orogenic type') peridotite bodies (Fig. 1); at least 17 of these bodies contain garnet-bearing assemblages, some spectacularly fresh and coarse grained (Eskola, 1921; Medaris, 1984; Carswell, 1986; Medaris & Carswell, 1990; Brueckner *et al.*, 2010).

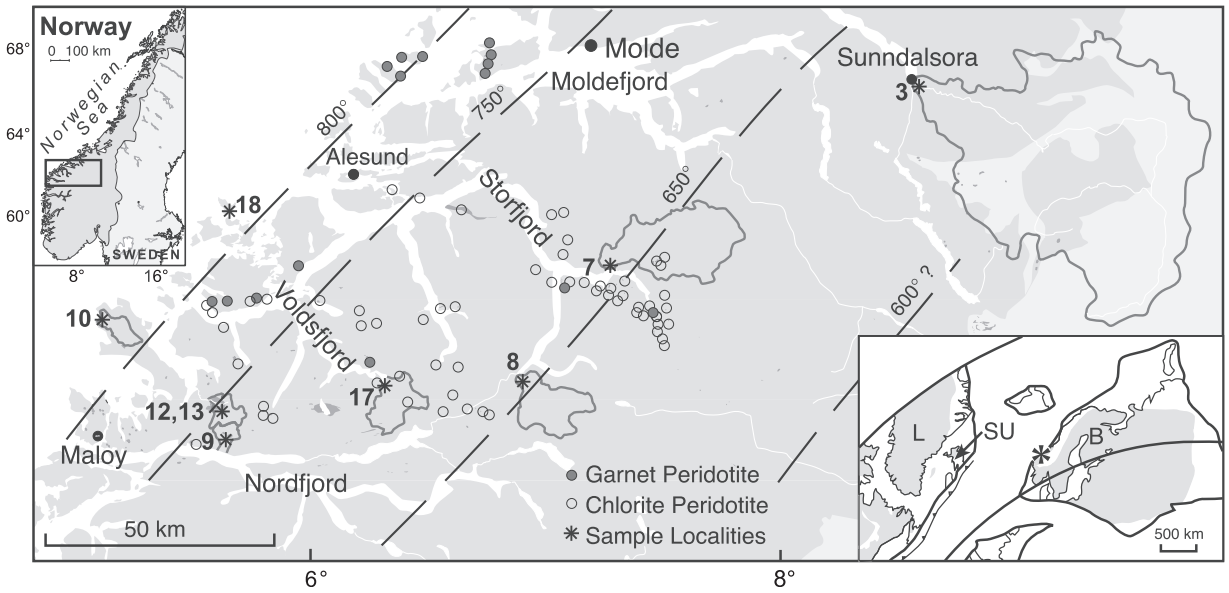

Fig. 1. Location map of the WGR showing drainage areas (outlined) with sampling localities (*); light grey shows allochthons. Dashed lines show generalized isotherms for the Caledonian HP–UHP metamorphism, derived from equilibration temperatures of eclogites (after Krogh, 1977, with additional data). The increasing T (and P) toward the coast should be noted; most of the UHP eclogites are found near, or west of, the 800°C isotherm. Open circles, small peridotite bodies; filled circles, localities with garnet peridotites. Almklovdalen peridotite bodies (areas 12 and 13) are omitted for clarity. Inset: tectonic reconstruction of the positions of Laurentia and Baltica *c.* 450 Myr ago (after Waldron *et al.*, 2008); SU, position of the Southern Uplands terrane studied by Waldron *et al.* (2008).

The collisional geometry described above provides a geometrically simple way of introducing these peridotite bodies into the gneisses of the WGR from the upper-mantle wedge above the subducted edge of Baltica (Brueckner, 1998). The garnetiferous assemblages have been dated by Sm–Nd and to a lesser extent by Lu–Hf mineral isochrons and give ages that stretch from *c.* 1·8 Ga to the Caledonian, with significant age clusters at *c.* 1·8, 1·0 and 0·43 Ga (Mearns, 1986; Jamtveit *et al.*, 1991; Brueckner *et al.*, 1996, 2002, 2010; Spengler *et al.*, 2006, 2009). These ages are similar to ages in the enclosing gneisses.

However, unlike the enclosing gneisses, these ultramafic rocks also preserve evidence of an evolution in the mantle that stretches back into the Archean. Re–Os dating of sulfides and whole-rock samples from the peridotites gives Archean model ages of *c.* 2·9–3·2 Ga (Brueckner *et al.*, 2002; Beyer *et al.*, 2004). These ages support ambiguous evidence for an Archean evolution obtained earlier by Lu–Hf and Sm–Nd studies of the garnet peridotites (Jamtveit *et al.*, 1991; Lapen *et al.*, 2005, 2009; Brueckner *et al.*, 2010) and garnet megacrysts within the peridotites (Spengler *et al.*, 2006). The apparent dilemma posed by these pre-Baltic Shield ages can be resolved if (1) the rocks of the SW Baltic Shield, and particularly of the WGR, contain Archean rocks (for example, in the deep crust) that have not yet been dated, or (2) the peridotites are exotic rocks that were derived not from beneath the Baltic Shield, but from beneath the Laurentian Shield (Beyer *et al.*, 2006), which has rocks of Archean age exposed at or near the east coast of Greenland.

SAMPLING

Samples were taken from drainage systems representing different portions of the WGR; one sample (Area 3, Fig. 1) may contain material from the adjacent allochthons. All known peridotite bodies occur north of Nordfjord and so sampling was restricted to drainage systems north of this fjord (Fig. 1). This sampling procedure assumes that the zircons were derived from lithologies within the drainage system and offers a reconnaissance method for dating magmatic and metamorphic events within terranes. The WGR has been heavily glaciated and it is natural to suspect that at least some zircons were transported long distances from other terranes and deposited with glacial till that was subsequently eroded. Although our results suggest that most zircons were locally derived, there remains the possibility that some were derived from adjacent drainage systems but give similar dates to those within the drainage system. These considerations are discussed further below.

Samples were taken from eight drainage systems, selected to provide a wide coverage of the northern portion of the WGR (Fig. 1, Table 1). Some desirable but steep drainages could not be sampled because the streams carry very little sand. Samples were collected where the trunk river of each drainage enters the sea (fjord) unless otherwise noted.

*Table 1: Sample location data**

Sample no.	Locality	Easting	Northing	Altitude (m)	Sediment type
N04-03	Sundalsøra	478326	6948477	7	river
N04-07	Valldal	409716	6908462	20	river
N04-08	Hellesylt	389266	6884680	7	river
N04-09	Nordfjord	324374	6872627	179	stream
N04-10	Stadlandet	297459	6898306	9	stream
N04-12	Gusdalsvatn	320746	6880622	52	river
N04-13	Lien	323470	6879193	117	stream
N04-17	Austefjord	360175	6883718	7	river
N04-18	Runde	326226	6921872	8	beach

*Co-ordinate system is UTM (WGS84) Zone 32V.

Sample N04-03 represents the large area drained by the Driva river. This drainage system reaches eastward into the Trondheim Basin and therefore samples the allochthonous units that occur there, as well as much of the northernmost WGR.

Sample N04-07 drains a north–south traverse from the lookout at the top of the Trollstigen road down to Valldal. The rocks are largely monotonous gneisses of the Jostedal Complex (i.e. parautochthonous Western Gneiss Complex; Bryhni & Grimstad, 1970).

Sample N04-08, collected just east of Hellesylt, represents an ENE–WSW cross-section that drains mostly gneisses of the Jostedal Complex. Sample N04-17 is from a roughly north–south drainage system that flows into Austefjord; like samples N04-07 and N04-08, it mostly samples the Jostedal Complex. Sample N04-09 was collected roughly halfway up a small river within a drainage system that flows south into Nordfjord, but unlike the eclogite-poor traverses to the east (i.e. N04-07 and N04-08) this drainage contains abundant eclogite as well as anorthosite, paragneiss, and mangerite (Young *et al.*, 2007). Similarly, sample N04-10 is from a stream that flows through an area with UHP eclogites and a large monzonite intrusion on the Stadlandet Peninsula.

Sample N04-18 was collected from the island of Runde off the coast south of Ålesund, within another UHP terrane interpreted to be allochthonous relative to the WGR basement; the exposed area consists largely of orthogneisses (Root *et al.*, 2005). The allochthonous rocks include quartzite, marble, calc-silicate gneiss, kyanite schist, augen gneiss, amphibolite and garnet-free peridotite, in addition to the UHP eclogites. This terrane thus is more heterogeneous than those represented by the other samples. Lithologically, it is very similar to the Fjordane Complex (Bryhni & Grimstad, 1970). There are no significant streams on these islands so sand was collected from a beach on the east side of the island.

Samples N04-12 and N04-13 were collected from the small Åheim river, which flows through the large Almklovdalen peridotite body with its spectacular outcrops of garnet peridotite, garnet pyroxenite (Medaris, 1984; Osland, 1997), and 'internal' eclogites (i.e. eclogites that occur within the peridotite; Griffin & Qvale, 1985). The dominant garnet-free peridotite consists of exceptionally fresh dunite and harzburgite (Osland, 1997; Beyer *et al.*, 2006) and is extensively quarried for refractory material. The enclosing rocks are heterogeneous orthogneiss, paragneiss and anorthosite, and 'external' eclogites occur within the gneisses. The N04-13 site is upstream from the quarries, but downstream from a small tributary with headwaters within the Lien garnet peridotite at Helgehornsvatn (Medaris, 1984), so some of the zircons have probably been derived from these outcrops. The sediments downstream of the main body (N04-12) were collected where the stream enters a lake (Gusdalvatn). These sediments contained abundant olivine and chromite derived from quarries upstream and offered the opportunity to sample zircons that may have been liberated from the peridotite during erosion and mining.

METHODS

The samples are heavy-mineral concentrates sieved or panned from river and stream sediments. Further concentration of these heavy minerals was carried out using a Wilfley table and heavy media separation. Zircons (100–150 grains per sample) were handpicked to provide a representative sampling of morphological populations as observed in the binocular microscope. Selected zircons from each sample were mounted in epoxy discs, which were then polished to expose the grains for analysis. A Camebax SX50 electron microprobe (EMP) was used to collect back-scattered electron (BSE) or cathodoluminescence (CL) images of the zircons and was also used to analyse the zircons for Si, Zr, Hf, Y, U and Th.

U–Pb dating of 50–65 grains from each sample was performed by laser ablation microprobe–inductively coupled plasma mass spectrometry (LAM-ICP-MS) using an HP 4500 series 300 ICP quadrupole MS system, attached to a New Wave 213 nm Nd:YAG laser; ablations were carried out in He. The analytical procedures for the U–Pb dating have been described in detail by Jackson *et al.* (2004). The GEMOC GJ-1 zircon was used as the primary standard, and zircon standards 91500 and Mud Tank were analyzed with each sample run as controls on precision and accuracy (in-run standard data for each sample are given as Supplementary Data, available for downloading at http://www.petrology.oxfordjournals.org). Single U–Pb ages were calculated from the raw signal data using the software package GLITTER (Griffin *et al.*, 2008).

Corrections for inherited ('common') Pb typically are based on the measurement of ^{204}Pb; this is not feasible in our LAM-ICP-MS technique because the Ar gas contains small amounts of Pb. The algorithm of Andersen (2002), which does not use ^{204}Pb to correct for common Pb, therefore was employed for this correction; grains requiring >2% correction were rejected. U and Th concentrations were calculated using the GEMOC GJ-1 zircon as an external standard.

The uncertainty calculations in the GLITTER software are based on standard uncertainty-propagation methods, with the assumption that raw data from the ICP-MS obey Poisson statistics. The uncertainty on standard values (in this case the well-characterized GJ-1 garnet) is set at 1%. The variance on total counts (T) in the integration interval is thus T, and the standard deviation is $\sqrt{T}$. This variance is propagated to the mean count rate ($m = T/n$, where n is the number of replicates in the integration interval), such that the variance in m is T/n^2. The standard deviation on m is then $(\sqrt{T})/n$. These variances are then propagated through all the subsequent equations using standard uncertainty-propagation methods, along with corrections for drift and yield.

Hf-isotope analyses were carried out *in situ* by LAM-ICP-MS using a New Wave Research LUV213 laser-ablation microprobe attached to a Nu Plasma multi-collector ICP-MS system. The analytical methods, and extensive data on the analysis of standard solutions and zircons, have been discussed in detail by Griffin *et al.* (2000, 2002). Concentrations of Lu and Yb were calculated from the Lu/Hf and Yb/Hf count-rate ratios collected during the Hf-isotope analysis, and known Hf concentrations from the EMP analysis. Two types of model ages can be calculated from the Hf-isotope data. T_{DM} model ages are calculated using the measured $^{176}Lu/^{177}Hf$ of the zircon grain, and give a minimum age for a potential juvenile source of the host magmatic rock. A more realistic 'crustal model age' (T_{DM}^{C}) can be calculated assuming that the source of the magma had the $^{176}Lu/^{177}Hf$ of the average continental crust (0·015; Griffin *et al.*, 2000). All calculations given here use the ^{176}Lu decay constant of Scherer *et al.* (2001).

The data collection routine is not dependent on a standard, but the Mud Tank standard zircon was analyzed several times with each sample as a control on precision and accuracy. Thirty-nine analyses gave a mean $^{176}Hf/^{177}Hf = 0{\cdot}282515 \pm 50$ (2SD); this is identical within error to the long-term average ($n = 2335$) for this standard in the GEMOC laboratory ($0{\cdot}282522 \pm 42$; Griffin *et al.*, 2007).

The zircons collected from drainages that tapped the Almklovdalen peridotite body (N04-12 and N04-13) were analyzed for trace elements because of their anomalously old ages (see below). Full trace-element data were collected for zircons from sample N04-12 during the U–Pb analysis, whereas the trace-element analyses of zircons from sample N04-13 were carried out in a separate ablation run, using a custom-built 266 nm Nd:YAG laser-ablation microsampling system attached to an Agilent 7500 ICP-MS system; ablations were carried out in He. In each case, the NIST-610 glass was used as the external standard, and Hf (measured by EMP) as the internal standard.

Rock-type analysis of zircons is based on a CART tree (similar to a botanical key) with a series of switches based on the levels of single elements or ratios (Belousova *et al.*, 2002). The 'short tree' was used for zircons from most of the drainage systems and is based on the trace elements (Hf, Y, U, Th, Lu, Yb) collected during the standard EMP, U–Pb and Hf-isotope analyses. This tree has been found to work well as a broad guide to rock composition (e.g. Belousova *et al.*, 2009), but the range of variability in zircon composition even within single rock samples means that the results must be interpreted carefully. Furthermore, rock types that were not represented in the database used to construct the discriminant tree must inevitably be misclassified. Nevertheless, as will be shown below, this approach can flag zircons that are derived from unusual rock types, such as ultramafic complexes. The 'long tree' of Belousova *et al.* (2002), which uses the rare earth elements (REE) in addition to Hf, Y, U, Th, Lu and Yb to discriminate rock types, was employed to classify the anomalously old zircons from samples N04-12 and N04-13, to take advantage of the full trace-element analyses carried out on these zircons.

ZIRCON MORPHOLOGY

The zircons in most WGR samples are clear grains that are sometimes colourless but more commonly are pale pink to pale orange. These grains are generally subhedral to euhedral in shape and vary in length from 50 to 250 μm (see Supplementary Data, Appendix 1). Rare grains >700 μm in length occur in most samples and commonly show some degree of rounding, indicative of either a protracted history for the zircon or long transport distances in rivers. These zircons are typically clear and either colourless or pink–orange. One sample (N04-10) contains a small population of yellow zircons that are subhedral to euhedral in shape and >150 μm in length. Oscillatory zoning was observed in many WGR zircons, although it is rarely well developed. Samples N04-12 and N04-13 contain a high proportion of grains that are essentially round (anhedral to subhedral) with variable development of facets, and uniform internal structures.

RESULTS

Zircon data (Table 2 and Supplementary Data, Appendix 2) are presented in figures as concordia plots (Fig. 2),

Table 2: U–Pb and Hf isotopic data for selected zircons

Sample	U-Pb ages							Hf isotopes						T_{DM}^{C}
	U (ppm)	Th/U	$^{207}Pb/^{206}Pb$	±2σ	$^{206}Pb/^{238}U$	±2σ	%disc	$^{176}Hf/^{177}Hf$	±2σ	$^{176}Lu/^{177}Hf$	±2σ	εHf	$Hf_{initial}$	
Sundalsøra (sample N04-03)														
N04-03-44	362	0·22	907	12	909	20	0·24	0·282144	0·000030	0·000640	0·000040	−2·57	0·282133	1·96
N04-03-14	89	1·78	961	16	959	20	−0·19	0·282106	0·000026	0·001283	0·000122	−3·15	0·282083	2·04
N04-03-57	43	0·49	977	42	984	16	0·70	0·282193	0·000028	0·000374	0·000020	1·03	0·282186	1·79
N04-03-45	64	0·46	1064	28	1057	28	−0·70	0·282177	0·000020	0·000474	0·000007	2·16	0·282167	1·78
N04-03-60	119	0·21	1214	14	1203	28	−1·05	0·281962	0·000016	0·000746	0·000050	−2·37	0·281945	2·18
N04-03-39	42	0·55	1312	24	1312	30	0·04	0·282177	0·000024	0·001266	0·000038	6·95	0·282146	1·66
N04-03-16	54	0·29	1464	14	1460	30	−0·28	0·282038	0·000022	0·000484	0·000082	6·09	0·282025	1·84
N04-03-07	73	0·35	1499	14	1499	34	−0·06	0·281780	0·000017	0·000417	0·000030	−2·22	0·281768	2·39
N04-03-48	168	0·40	1530	12	1529	34	−0·02	0·281841	0·000024	0·002334	0·000060	−1·33	0·281773	2·36
N04-03-17	123	0·63	1553	10	1550	30	−0·19	0·281907	0·000016	0·000994	0·000050	2·89	0·281878	2·11
N04-03-52	437	0·62	1606	12	1604	34	−0·18	0·281872	0·000017	0·000758	0·000122	3·07	0·281849	2·14
N04-03-01	53	0·51	1628	14	1628	34	−0·01	0·281933	0·000026	0·001017	0·000032	5·43	0·281902	2·01
N04-03-06	118	0·96	1658	10	1657	34	−0·06	0·281869	0·000020	0·000678	0·000018	4·20	0·281848	2·11
N04-03-36	107	0·60	1684	10	1681	34	−0·12	0·281818	0·000015	0·000868	0·000062	2·75	0·281790	2·22
N04-03-38	237	0·56	1712	12	1712	36	0·02	0·281838	0·000026	0·001121	0·000100	3·79	0·281802	2·18
Valldal (sample N04-07)														
N04-07-05	36	0·45	894	36	888	20	−0·67	0·282171	0·000034	0·000506	0·000020	−1·95	0·282163	1·90
N04-07-16	72	0·67	912	28	931	12	2·16	0·282146	0·000026	0·000361	0·000032	−1·80	0·282140	1·93
N04-07-35	13	0·00	989	110	983	30	−0·63	0·282097	0·000010	0·000089	0·000022	−2·08	0·282095	1·99
N04-07-58	217	0·07	1342	6	1303	18	−3·21	0·281842	0·000013	0·001301	0·000048	−4·31	0·281809	2·41
N04-07-07	139	0·40	1553	10	1534	18	−1·36	0·281817	0·000036	0·000975	0·000056	−0·28	0·281788	2·31
N04-07-40	100	0·54	1562	14	1569	20	0·54	0·281937	0·000024	0·000408	0·000009	4·77	0·281925	2·00
N04-07-27	139	0·76	1584	12	1576	34	−0·50	0·281919	0·000024	0·002098	0·000380	2·82	0·281856	2·14
N04-07-57	136	0·57	1612	12	1614	34	0·12	0·281886	0·000019	0·000549	0·000014	3·92	0·281869	2·09
N04-07-25	102	0·99	1623	12	1616	34	−0·45	0·281860	0·000038	0·000816	0·000042	2·95	0·281835	2·16
N04-07-28	112	0·61	1649	12	1647	34	−0·09	0·281875	0·000024	0·001170	0·000082	3·67	0·281838	2·14
N04-07-33	333	0·63	1652	12	1652	34	0·02	0·281867	0·000018	0·001230	0·000074	3·38	0·281829	2·16
N04-07-85	160	0·60	1668	12	1663	36	−0·34	0·281838	0·000019	0·000810	0·000082	3·17	0·281812	2·18
N04-07-29	193	0·59	1681	12	1688	36	0·50	0·281834	0·000020	0·001325	0·000122	2·74	0·281792	2·22
N04-07-13	304	0·52	1688	10	1687	34	0·01	0·281816	0·000022	0·000807	0·000040	2·84	0·281790	2·22
N04-07-20	126	0·47	1695	12	1693	36	−0·17	0·281850	0·000015	0·000510	0·000013	4·54	0·281834	2·12
Hellesylt (sample N04-08)														
N04-08-20R	2989	0·01	411	12	408	8	−0·83	0·282161	0·000017	0·001327	0·000130	−13·02	0·282151	2·23
N04-08-68	59	1·34	868	20	849	16	−2·31	0·282069	0·000022	0·000597	0·000034	−6·47	0·282059	2·16
N04-08-121	44	1·19	930	17	879	16	−5·87	0·282074	0·000024	0·000635	0·000030	−5·67	0·282064	2·13
N04-08-79	65	0·98	939	15	882	16	−6·55	0·282087	0·000016	0·000643	0·000030	−5·14	0·282076	2·10
N04-08-48C	36	1·28	941	21	893	18	−5·51	0·282078	0·000014	0·000739	0·000050	−5·29	0·282066	2·12
N04-08-96	380	1·38	911	10	839	16	−8·51	0·282054	0·000028	0·001204	0·000086	−7·57	0·282035	2·22
N04-08-18	121	0·74	945	11	902	18	−4·97	0·282080	0·000019	0·000612	0·000064	−4·94	0·282070	2·10
N04-08-91C	64	1·19	952	15	885	16	−7·57	0·282091	0·000014	0·000574	0·000020	−4·89	0·282081	2·09
N04-08-21	166	1·11	960	9	935	16	−2·83	0·282075	0·000018	0·000434	0·000056	−4·28	0·282067	2·09
N04-08-33C	470	0·003	973	11	941	18	−3·58	0·282139	0·000010	0·001134	0·000158	−2·32	0·282119	1·97
N04-08-76	105	1·07	971	11	943	16	−3·09	0·282071	0·000022	0·000517	0·000018	−4·30	0·282062	2·09

(continued)

Table 2: Continued

Sample	U–Pb ages							Hf isotopes						T_{DM}^{C}
	U (ppm)	Th/U	$^{207}Pb/^{206}Pb$	±2σ	$^{206}Pb/^{238}U$	±2σ	%disc	$^{176}Hf/^{177}Hf$	±2σ	$^{176}Lu/^{177}Hf$	±2σ	εHf	$Hf_{initial}$	
N04-08-17	66	1·24	971	17	952	18	−2·15	0·282080	0·000024	0·000551	0·000036	−3·80	0·282070	2·07
N04-08-94	151	0·54	1390	25	1352	24	−3·02	0·281933	0·000024	0·000706	0·000022	2·46	0·281913	2·08
N04-08-13	122	0·99	1442	64	1390	30	−4·03	0·281920	0·000030	0·000504	0·000060	−7·74	0·282002	2·27
N04-08-61	213	0·34	1481	11	1401	26	−5·99	0·281963	0·000022	0·000859	0·000019	3·42	0·281939	2·02
Nordfjord (sample N04-09)														
N04-09-37	176	0·43	902	14	898	18	−0·47	0·282225	0·000024	0·000567	0·000013	0·23	0·282215	1·78
N04-09-29	98	0·66	942	22	926	20	−1·86	0·282127	0·000024	0·000942	0·000088	−2·60	0·282110	1·99
N04-09-38	120	1·26	985	14	982	18	−0·35	0·282019	0·000028	0·000935	0·000048	−5·49	0·282002	2·20
N04-09-22	78	1·30	1016	16	1014	18	−0·27	0·281881	0·000019	0·001719	0·000058	−10·24	0·281848	2·53
N04-09-60	259	0·61	1050	14	1037	22	−1·34	0·282047	0·000024	0·000722	0·000068	−2·93	0·282033	2·09
N04-09-72	37	0·47	1134	16	1116	22	−1·78	0·282099	0·000026	0·000536	0·000026	0·89	0·282088	1·91
N04-09-04	60	0·64	1172	16	1171	22	0·01	0·282085	0·000018	0·000705	0·000088	1·10	0·282069	1·93
N04-09-16	243	0·26	1369	8	1321	12	−3·87	0·281911	0·000024	0·001436	0·000168	−1·40	0·281874	2·24
N04-09-81	269	0·44	1385	12	1369	16	−1·24	0·282284	0·000038	0·000420	0·000052	13·12	0·282273	1·32
N04-09-70	121	0·58	1424	18	1414	18	−0·79	0·281794	0·000022	0·000904	0·000026	−3·86	0·281770	2·44
N04-09-77	133	0·46	1482	10	1434	24	−3·63	0·281983	0·000019	0·000732	0·000026	4·29	0·281962	1·97
N04-09-20	157	0·49	1556	10	1554	28	−0·23	0·281841	0·000019	0·000910	0·000040	0·70	0·281814	2·25
N04-09-23	340	0·78	1643	10	1661	26	1·27	0·282097	0·000024	0·000570	0·000144	12·08	0·282079	1·59
N04-09-42	252	0·64	1648	8	1644	24	−0·21	0·281814	0·000017	0·002154	0·000104	0·39	0·281747	2·34
N04-09-48	95	0·65	1662	10	1656	26	−0·40	0·281832	0·000022	0·001086	0·000034	2·52	0·281798	2·22
Stadlandet (sample N04-10)														
N04-10-36	162	0·34	1521	24	1460	30	−4·53	0·281868	0·000017	0·001526	0·000120	0·26	0·281824	2·25
N04-10-35	66	0·72	1541	44	1522	32	−1·34	0·281884	0·000017	0·001228	0·000120	1·57	0·281848	2·19
N04-10-30	422	0·30	1553	24	1508	30	−3·30	0·281832	0·000014	0·000987	0·000028	0·24	0·281803	2·28
N04-10-24	102	0·83	1581	18	1574	30	−0·50	0·281877	0·000018	0·001187	0·000040	2·23	0·281841	2·17
N04-10-40	521	0·23	1595	18	1594	32	−0·06	0·281835	0·000018	0·001299	0·000160	0·93	0·281796	2·27
N04-10-11	103	0·59	1597	10	1594	28	−0·23	0·281821	0·000015	0·001066	0·000164	0·73	0·281789	2·28
N04-10-20	420	0·11	1600	18	1590	32	−0·73	0·281801	0·000014	0·001014	0·000048	0·14	0·281770	2·32
N04-10-33	105	0·53	1600	18	1599	30	−0·03	0·281815	0·000016	0·000936	0·000016	0·72	0·281787	2·29
N04-10-03	414	1·04	1603	10	1598	26	−0·33	0·281874	0·000024	0·000885	0·000016	2·93	0·281847	2·15
N04-10-42	266	0·77	1606	22	1599	32	−0·52	0·281840	0·000022	0·000785	0·000032	1·90	0·281816	2·22
N04-10-34	148	0·43	1612	16	1610	28	−0·08	0·281824	0·000013	0·000757	0·000018	1·50	0·281801	2·25
N04-10-29	114	0·75	1620	16	1599	28	−1·42	0·281832	0·000019	0·000921	0·000106	1·78	0·281804	2·23
N04-10-37	399	0·21	1628	18	1620	32	−0·57	0·281864	0·000018	0·001870	0·000082	2·05	0·281806	2·22
N04-10-31	90	0·63	1646	22	1642	32	−0·31	0·281783	0·000018	0·001023	0·000022	0·50	0·281751	2·34
N04-10-22	322	0·66	1674	22	1622	32	−3·57	0·281804	0·000017	0·001460	0·000092	1·37	0·281758	2·30
Gusdalsvatn (sample N04-12)														
N04-12-78	430	0·03	427	44	396	10	−7·54	0·281591	0·000058	−0·000156	0·000007	−33·06	0·281592	3·46
N04-12-44	275	1·47	965	30	947	22	−2·07	0·282101	0·000024	0·000431	0·000044	−3·10	0·282093	2·02
N04-12-48	1862	0·59	1182	36	1197	28	1·39	0·282148	0·000022	0·001767	0·000240	2·71	0·282109	1·83
N04-12-72	632	0·60	1399	28	1030	24	−28·5	0·282107	0·000022	0·000224	0·000046	7·33	0·282101	1·71
N04-12-69	200	0·41	1484	34	1492	34	0·59	0·281973	0·000014	0·000553	0·000018	4·15	0·281957	1·98
N04-12-97	112	0·46	1502	28	1439	30	−4·73	0·281931	0·000022	0·000876	0·000024	2·75	0·281906	2·08
N04-12-73	310	0·96	1535	30	1500	34	−2·56	0·281930	0·000022	0·001447	0·000018	2·84	0·281888	2·10

(continued)

Table 2: Continued

Sample	U–Pb ages							Hf isotopes						T_{DM}^{C}
	U (ppm)	Th/U	$^{207}Pb/^{206}Pb$	±2σ	$^{206}Pb/^{238}U$	±2σ	%disc	$^{176}Hf/^{177}Hf$	±2σ	$^{176}Lu/^{177}Hf$	±2σ	εHf	$Hf_{initial}$	
N04-12-147	171	0·49	1572	24	1507	32	−4·7	0·281940	0·000015	0·000856	0·000007	4·63	0·281915	2·01
N04-12-77C	245	1·17	1613	32	1607	36	−0·40	0·281843	0·000016	0·000957	0·000022	1·97	0·281814	2·22
N04-12-32	96	0·41	1757	28	1888	42	8·60	0·281597	0·000024	0·000480	0·000008	−3·03	0·281581	2·65
N04-12-92	237	1·35	2247	32	1945	44	−15·55	0·281446	0·000038	0·000025	0·000003	3·33	0·281445	2·62
N04-12-196	371	0·49	2534	26	1766	38	−34·58	0·280990	0·000034	0·000302	0·000019	−6·75	0·280975	3·48
N04-12-124C	196	0·43	2608	24	2025	48	−25·21	0·281325	0·000028	0·000373	0·000028	6·74	0·281306	2·68
N04-12-122	434	0·54	2668	34	2619	54	−2·27	0·281089	0·000028	0·001162	0·000054	−1·72	0·281030	3·27
N04-12-140C	315	0·26	2753	20	2406	48	−15·09	0·281222	0·000032	0·000525	0·000044	6·10	0·281194	2·83
Lien (sample N04-13)														
N04-13-44	72	0·43	589	66	585	12	−0·61	0·282120	0·000011	0·000554	0·000030	−10·41	0·282114	2·20
N04-13-61	5	0·06	683	316	678	34	−0·79	0·280979	0·000013	0·000245	0·000016	−48·65	0·280976	4·62
N04-13-27	418	0·29	840	32	817	16	−2·95	0·282008	0·000012	0·000355	0·000003	−8·69	0·282002	2·29
N04-13-33	47	0·51	1015	82	1023	24	0·93	0·282087	0·000022	0·002477	0·000146	−3·47	0·282040	2·10
N04-13-37	39	1·30	1200	20	1196	22	−0·34	0·282021	0·000012	0·000573	0·000024	−0·45	0·282008	2·05
N04-13-06	76	0·28	1413	22	1415	28	0·18	0·282001	0·000015	0·000487	0·000050	3·64	0·281988	1·95
N04-13-55	172	0·39	1503	14	1500	24	−0·25	0·281933	0·000028	0·000628	0·000052	3·08	0·281915	2·06
N04-13-08	61	0·98	1644	68	1654	32	0·65	0·281032	0·000018	0·000018	0·000002	−25·09	0·281031	3·94
N04-13-24	260	0·12	2673	16	2671	42	−0·13	0·281036	0·000017	0·000004	0·000000	−1·39	0·281036	3·25
N04-13-14	195	0·63	2676	20	2562	52	−5·16	0·280985	0·000012	0·000450	0·000012	−3·95	0·280962	3·41
N04-13-53	48	0·52	2685	26	2619	46	−2·99	0·281003	0·000022	0·000943	0·000070	−4·01	0·280955	3·42
N04-13-04	197	0·18	2703	18	2565	44	−6·20	0·281045	0·000015	0·000323	0·000100	−0·97	0·281028	3·24
N04-13-34	94	0·86	2753	20	2739	60	−0·66	0·281008	0·000010	0·000018	0·000003	−0·56	0·281007	3·26
N04-13-88	77	0·72	2762	16	2761	50	−0·03	0·281040	0·000016	0·000038	0·000003	0·75	0·281038	3·18
N04-13-83	42	0·39	2809	14	2720	42	−3·88	0·280922	0·000013	0·000047	0·000008	−2·38	0·280919	3·42
Austefjord (sample N04-17)														
N04-17-38	90	0·01	415	30	412	8	−0·78	0·282182	0·000016	0·000090	0·000026	−11·84	0·282181	2·16
N04-17-57	37	1·66	905	26	874	18	−3·70	0·282050	0·000019	0·000357	0·000012	−6·46	0·282044	2·18
N04-17-61	35	1·62	934	22	930	18	−0·38	0·282111	0·000016	0·000562	0·000070	−3·19	0·282101	2·01
N04-17-80	64	1·26	957	20	951	16	−0·66	0·282037	0·000011	0·000486	0·000013	−4·75	0·282028	2·15
N04-17-23	33	0·10	1086	20	1082	20	−0·36	0·282163	0·000016	0·000278	0·000015	2·29	0·282157	1·79
N04-17-09	61	0·57	1193	18	1192	20	−0·12	0·282099	0·000014	0·000808	0·000042	1·98	0·282081	1·89
N04-17-30	64	0·42	1385	46	1354	30	−2·48	0·282014	0·000014	0·000838	0·000056	3·15	0·281992	1·96
N04-17-55	201	0·61	1422	44	1423	30	0·11	0·281868	0·000022	0·000873	0·000080	−1·23	0·281845	2·27
N04-17-70	181	0·60	1487	40	1478	34	−0·62	0·281897	0·000022	0·000922	0·000034	1·16	0·281871	2·17
N04-17-08	65	0·67	1503	42	1490	30	−0·97	0·280507	0·000017	0·000309	0·000009	−47·48	0·280498	5·19
N04-17-39	55	0·74	1564	18	1539	26	1·81	0·281877	0·000017	0·000605	0·000026	2·47	0·281859	2·15
N04-17-74	218	0·36	1597	16	1598	28	0·02	0·281883	0·000011	0·000310	0·000098	3·74	0·281874	2·09
N04-17-28	189	0·60	1610	14	1607	26	−0·16	0·281893	0·000022	0·001177	0·000106	3·45	0·281857	2·12
N04-17-32	171	0·60	1637	18	1634	28	−0·25	0·281878	0·000016	0·001011	0·000086	3·69	0·281847	2·12
N04-17-35	134	0·47	1676	18	1663	30	−0·91	0·281863	0·000018	0·001562	0·000062	3·39	0·281813	2·17
Runde (sample N04-18)														
N04-18-75	235	1·29	924	22	847	14	−8·91	0·282084	0·000020	0·000608	0·000042	−6·00	0·282074	2·13
N04-18-95	16	1·19	956	92	868	20	−9·77	0·282045	0·000016	0·000327	0·000010	−4·82	0·282039	2·14
N04-18-96	13	1·77	903	80	897	18	−0·68	0·282045	0·000012	0·000438	0·000011	−6·05	0·282038	2·17

(continued)

Table 2: Continued

Sample	U–Pb ages							Hf isotopes						T_{DM}^{C}
	U (ppm)	Th/U	$^{207}Pb/^{206}Pb$	±2σ	$^{206}Pb/^{238}U$	±2σ	%disc	$^{176}Hf/^{177}Hf$	±2σ	$^{176}Lu/^{177}Hf$	±2σ	εHf	$Hf_{initial}$	
N04-18-39	107	1·74	937	20	907	16	−3·48	0·282106	0·000016	0·000801	0·000104	−4·03	0·282092	2·05
N04-18-21	171	2·09	945	28	914	20	−3·56	0·282158	0·000028	0·000421	0·000086	−1·80	0·282151	1·91
N04-18-46	81	1·23	965	35	930	18	−3·94	0·282092	0·000017	0·000714	0·000046	−3·95	0·282080	2·06
N04-18-03	22	1·47	971	56	939	20	−3·56	0·282078	0·000026	0·000410	0·000007	−4·07	0·282071	2·08
N04-18-98	87	1·08	945	30	948	16	0·32	0·282070	0·000017	0·000543	0·000007	−4·30	0·282060	2·10
N04-18-79	209	0·35	1351	50	1211	22	−11·42	0·281947	0·000038	0·000902	0·000068	0·87	0·281923	2·12
N04-18-27	642	0·35	1456	50	1253	22	−15·36	0·281939	0·000015	0·000877	0·000030	6·18	0·281912	1·97
N04-18-59	386	0·07	1580	18	1240	22	−23·59	0·282058	0·000019	0·000223	0·000034	2·09	0·282053	1·92
N04-18-54	329	0·67	1584	18	1376	24	−14·58	0·282027	0·000024	0·000553	0·000106	8·29	0·282010	1·79
N04-18-19	830	0·10	1606	22	1403	26	−14·1	0·281824	0·000019	0·000838	0·000062	1·53	0·281798	2·25
N04-18-52	131	0·64	1668	22	1585	26	−5·60	0·281910	0·000016	0·002288	0·000164	4·07	0·281838	2·12
N04-18-08	951	0·47	1889	18	1731	30	−9·56	0·281723	0·000024	0·001657	0·000126	−0·51	0·281669	2·47

as probability-density plots of concordant U–Pb ages (Fig. 3), as $^{176}Hf/^{177}Hf_{initial}$ ratios vs age (note that $^{176}Hf/^{177}Hf_{measured} = {}^{176}Hf/^{177}Hf_{initial}$; Fig. 4 and Supplementary Data) and as εHf_t vs age (Fig. 5). Data points in Figs 4 and 5 are labeled according to rock type. The zircon ages show the WGR to be a complex terrane with two major periods of tectonothermal activity (Mesoproterozoic and Neoproterozoic), overprinted by Caledonian HP–UHP metamorphism. Archean ages occur only in drainage systems that contain peridotite bodies. As a result of this multiple overprinting, most zircons show varying degrees of discordance but simple linear discordia arrays are rare.

Fortunately, Hf-isotope data are invaluable for bringing order to an apparently chaotic distribution of U–Pb ages characterized by poorly defined discordia lines. The systematics of U–Pb/Hf isotope data in magmatic and metamorphosed zircon have been discussed in detail by Amelin *et al.* (2000). A similar investigation was carried out on mantle zircons from eclogitic xenoliths by Schmidberger *et al.* (2005). Both studies pointed out that the diffusion rates of Lu and Hf in the zircon lattice are extremely slow under any geologically reasonable conditions, even at high temperatures, making it difficult to reset the Hf-isotope composition of a zircon. Mass-balance considerations add a further constraint, as in most rocks essentially all of the Hf in the rock is locked in zircon. Hence interaction of the zircon with the Hf-poor matrix during metamorphic events can produce little change in the $^{176}Hf/^{177}Hf$ of the zircon. An elegant illustration of this principle has been provided by Lauri *et al.* (2011), who showed that 3·7 Ga magmatic zircons in rocks metamorphosed to granulite facies at 2·7 Ga experienced variable to complete resetting of their U–Pb ages, but no change in their Hf-isotope ratios.

Therefore a plot of U–Pb age vs Hf-isotope composition ($^{176}Hf/^{177}Hf_i$) will show that zircons that have undergone non-zero Pb loss (i.e. those lying on discordia with lower intercepts >0) will scatter along horizontal trends extending from their 'real' ages toward the younger (but meaningless) $^{207}Pb/^{206}Pb$ ages, at constant $^{176}Hf/^{177}Hf$ (Fig. 4). This aspect of the systematics makes Hf isotope analysis an invaluable adjunct to U–Pb dating, especially in complex terrains (e.g. Amelin *et al.*, 2000). Therefore the discussion of the results given here does not follow the conventional sequential presentation of the various types of data, but focuses on the integrated interpretation of the datasets from each sample, as summarized in Figs 4 and 5.

N04-03 (Sundalsøra)

The analyzed zircons mainly scatter along the concordia (Fig. 2a); only a few grains are significantly discordant. The probability-density plot of concordant ages (Fig. 3a) shows a major peak at 1·65 Ga, and a scatter of ages to as young as *c.* 900 Ma. The plot of $^{176}Hf/^{177}Hf_i$ vs age (Fig. 4a) resolves these data into two populations, each showing some non-zero Pb loss. The older population centers on ages of 1·65–1·79 Ga, with $\varepsilon Hf_t = +3$ to +10 (Fig. 5a), but includes a few grains as young as 950 Ma. The oldest grains in the younger population have ages of 1·28–1·31 Ma, and $\varepsilon Hf_t = +5$ to +8; reset ages extend to as young as 900 Ma. The lower εHf_t values for apparently younger grains from each population reflect the resetting of the U–Pb system; thus only the maximum values, in the oldest grains of each population, represent the original

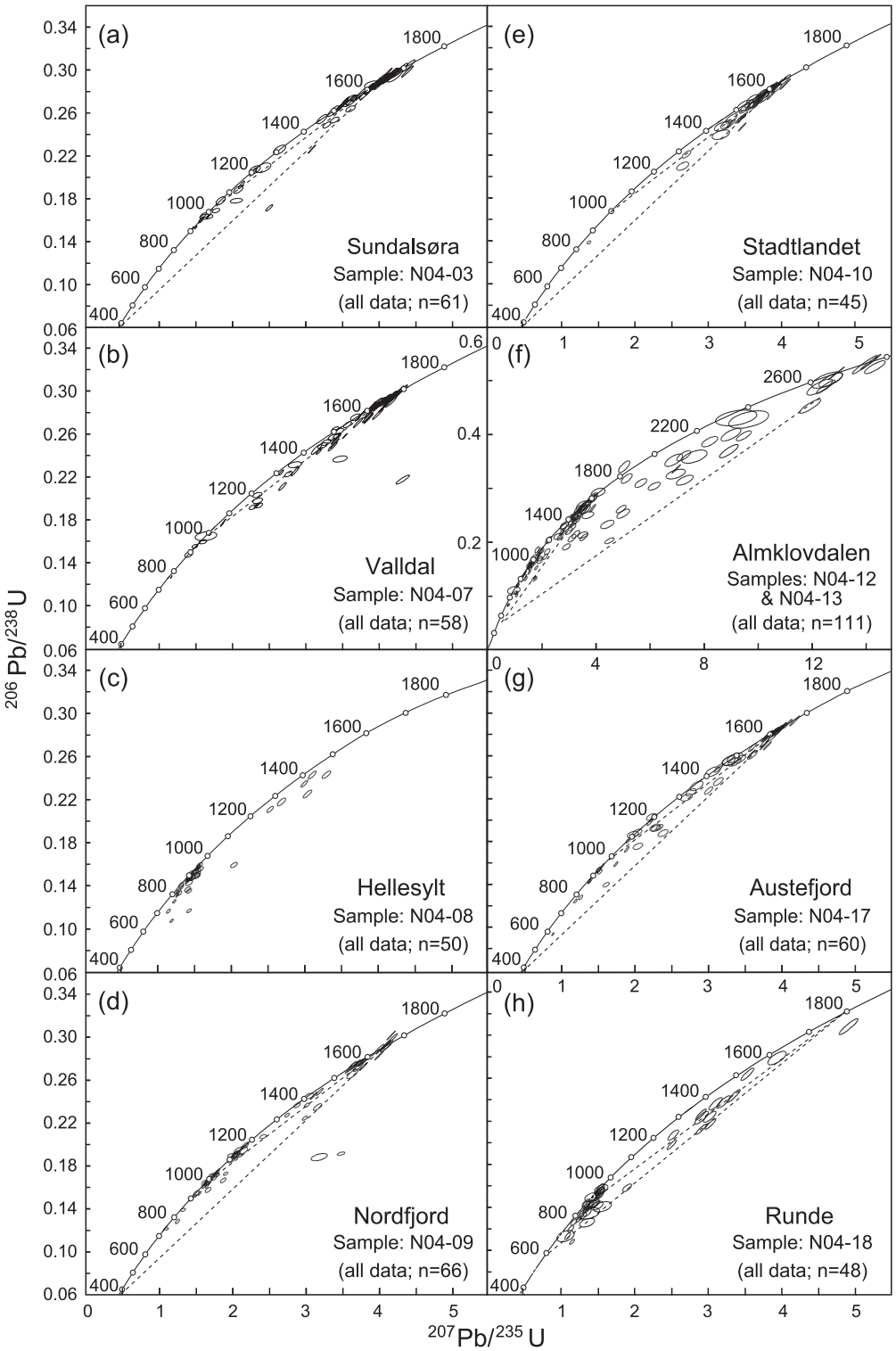

Fig. 2. Concordia plots of U–Pb data for zircons from each locality. The dashed lines represent non-zero Pb loss during the *c.* 1·0 Ga Sveconorwegian Orogeny and the *c.* 400 Ma Scandian Orogeny.

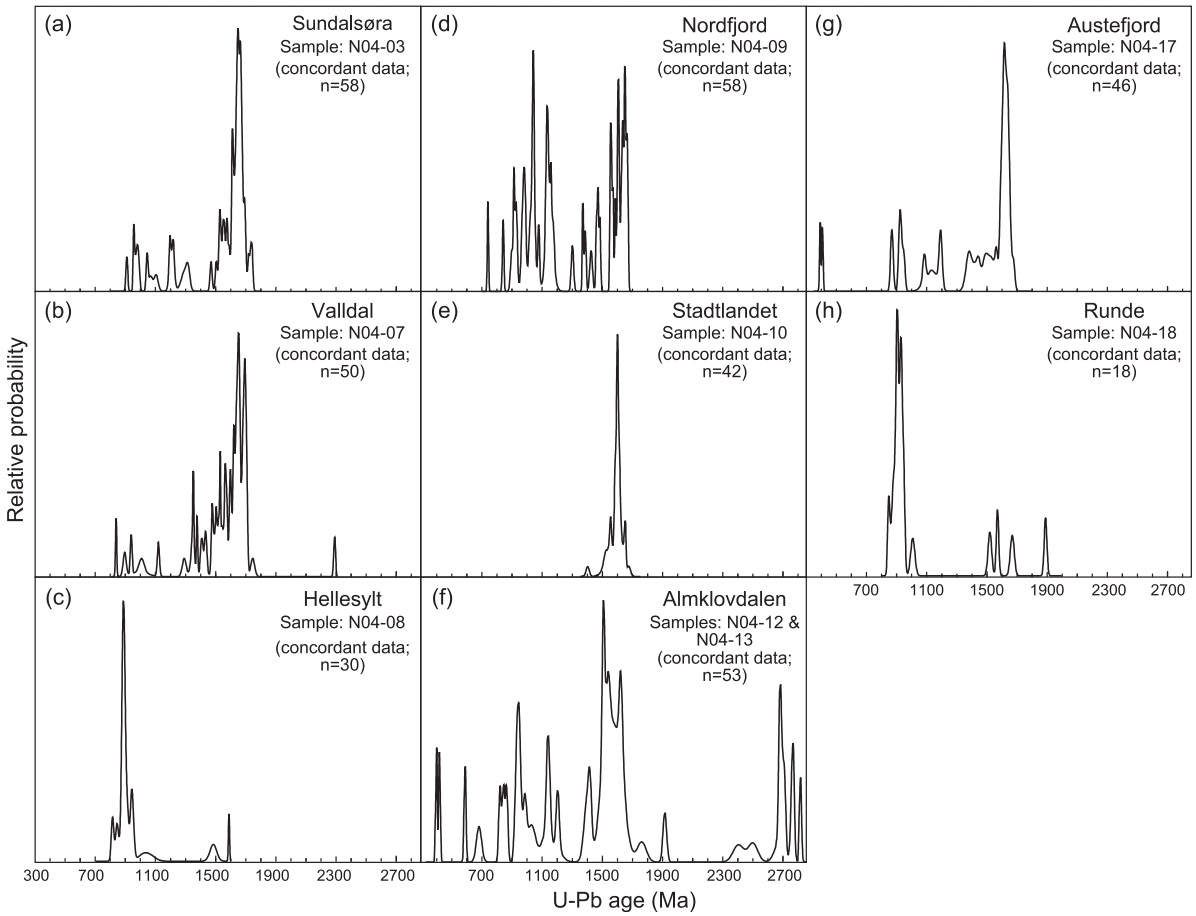

Fig. 3. Cumulative-probability plots of the U–Pb ages for concordant or near-concordant zircons from each sample. Discordant 'ages' are not plotted because they may reflect non-zero Pb loss and hence are meaningless. Ages <1 Ga are $^{206}Pb/^{238}U$ ages; ages >1 Ga are $^{207}Pb/^{206}Pb$ ages.

magmatic $^{176}Hf/^{177}Hf_i$. The older population is equally divided among zircons typical of high-Si granitoids, low-Si granitoids and mafic rocks, whereas the younger population is dominated by zircons typical of mafic rocks. The river that flows into Sundalsøra drains the allochthonous terranes (the Middle and Upper Allochthon) of the Trondheim Basin, yet the age patterns are very similar to those of zircons derived from the rest of the WGR. This similarity is consistent with the generally accepted origin of the Middle Allochthon from the western margin of Baltica, but it is curious that mid-Paleozoic ages typical of the oceanic Upper Allochthon are sparse.

N04-07 (Valldal)

Most of the data points are concordant, with $^{207}Pb/^{206}Pb$ ages of 1·6–1·7 Ga or 900–1000 Ma (Fig. 2b); however, a significant proportion scatters around a poorly defined discordia line between 1·65 and 1·0 Ga. The probability-density plot (Fig. 3b) of the concordant data shows two major peaks between 1·6 and 1·7 Ga, and a broad scatter to younger ages. The $^{176}Hf/^{177}Hf_i$ –age plot (Fig. 4b) resolves these data into an older population centered around 1·68 Ga; non-zero Pb loss is apparent in the horizontal distribution of data points, with one grain reset to 830 Ma. The younger population, with $\varepsilon Hf_t = -1$ to $-2{\cdot}5$, contains only four grains, all derived from mafic sources (open diamonds); the oldest is 1·0 Ga. One grain at 1·11 Ga could belong to either population. The older population, with $\varepsilon Hf_t = +4$ to $+6$ (one grain at $\varepsilon Hf_t = +11$; Fig. 5b), contains zircons typical of a range of granitoids (circles and triangles) and mafic rocks. There was some resetting by the Caledonian orogeny but it appears to be relatively minimal in this terrane. One zircon with an apparent U–Pb age of 2·2 Ga falls well below the others ($\varepsilon Hf_t = -13$, Fig. 5b) and has an Archean model age. Data from other samples (see below) suggest that this zircon may have been derived from a large peridotite body (Trollkirke locality) that occurs in the Valldal drainage.

N04-08 (Hellesylt)

A large population of grains is concordant with ages of 850–1050 Ma (Fig. 2c); a tail of discordant grains extends

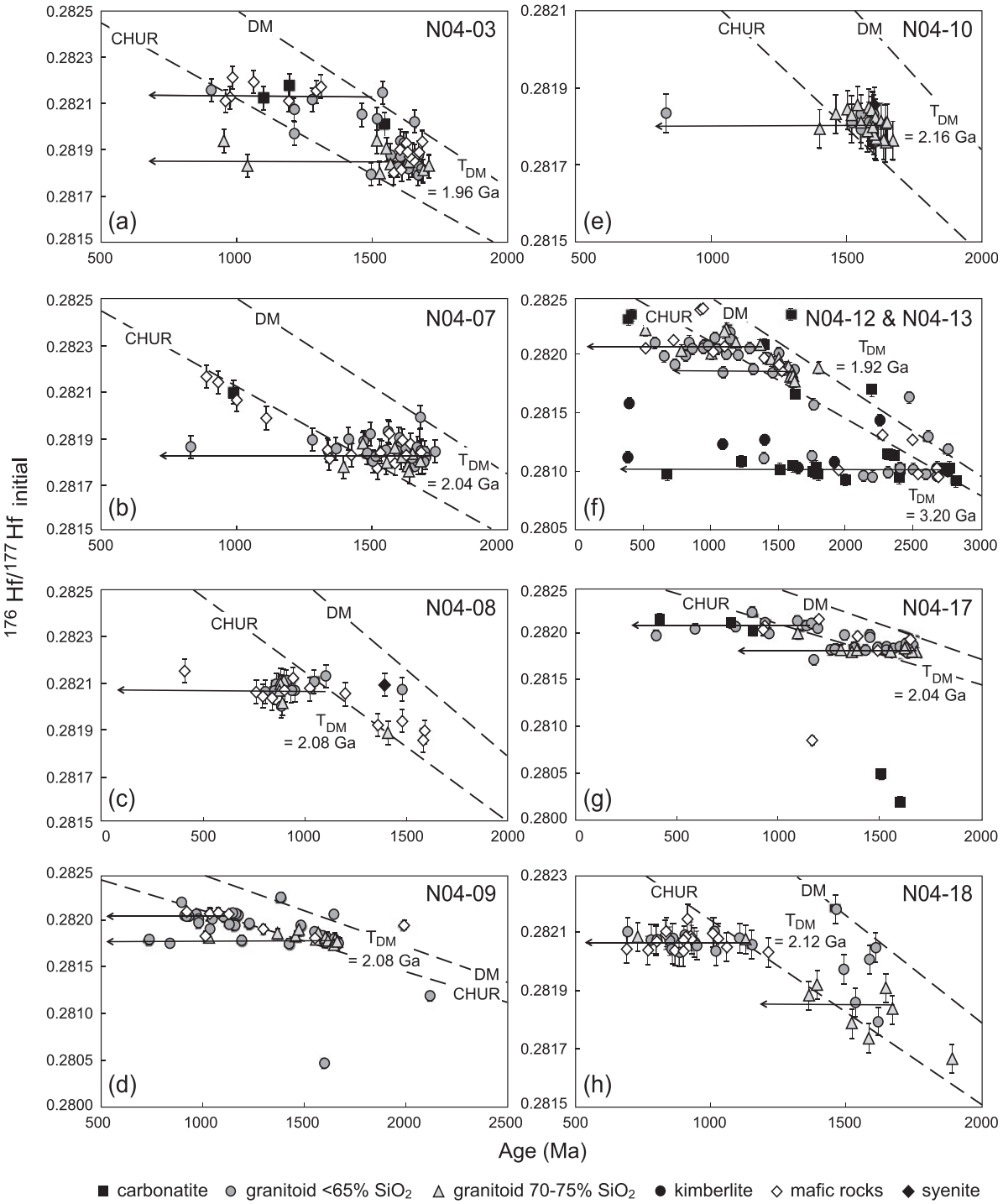

Fig. 4. Plots of $^{176}Hf/^{177}Hf_i$ vs age for zircons from each locality. Ages <1 Ga are $^{206}Pb/^{238}U$ ages; ages >1 Ga are $^{207}Pb/^{206}Pb$ ages. Dashed lines are continental evolution lines calculated using the mean crustal $^{176}Lu/^{177}Hf = 0{\cdot}015$. Horizontal arrows indicate Pb loss during younger thermal events, without change in Hf-isotope composition. Error bars are ±0·00005 (2σ level uncertainty).

from this cluster toward younger ages. A few more discordant analyses give Mesoproterozoic ages; three of these represent cores in grains whose rims fall in the younger population. One Caledonian age (400 Ma) was obtained from the rim of a grain whose core gives an age of 1·58 Ga. The probability-density plot (Fig. 3c) shows a major Neoproterozoic peak (885 Ma). In the $^{176}Hf/^{177}Hf_i$–age plot (Fig. 4c) the younger population shows significant

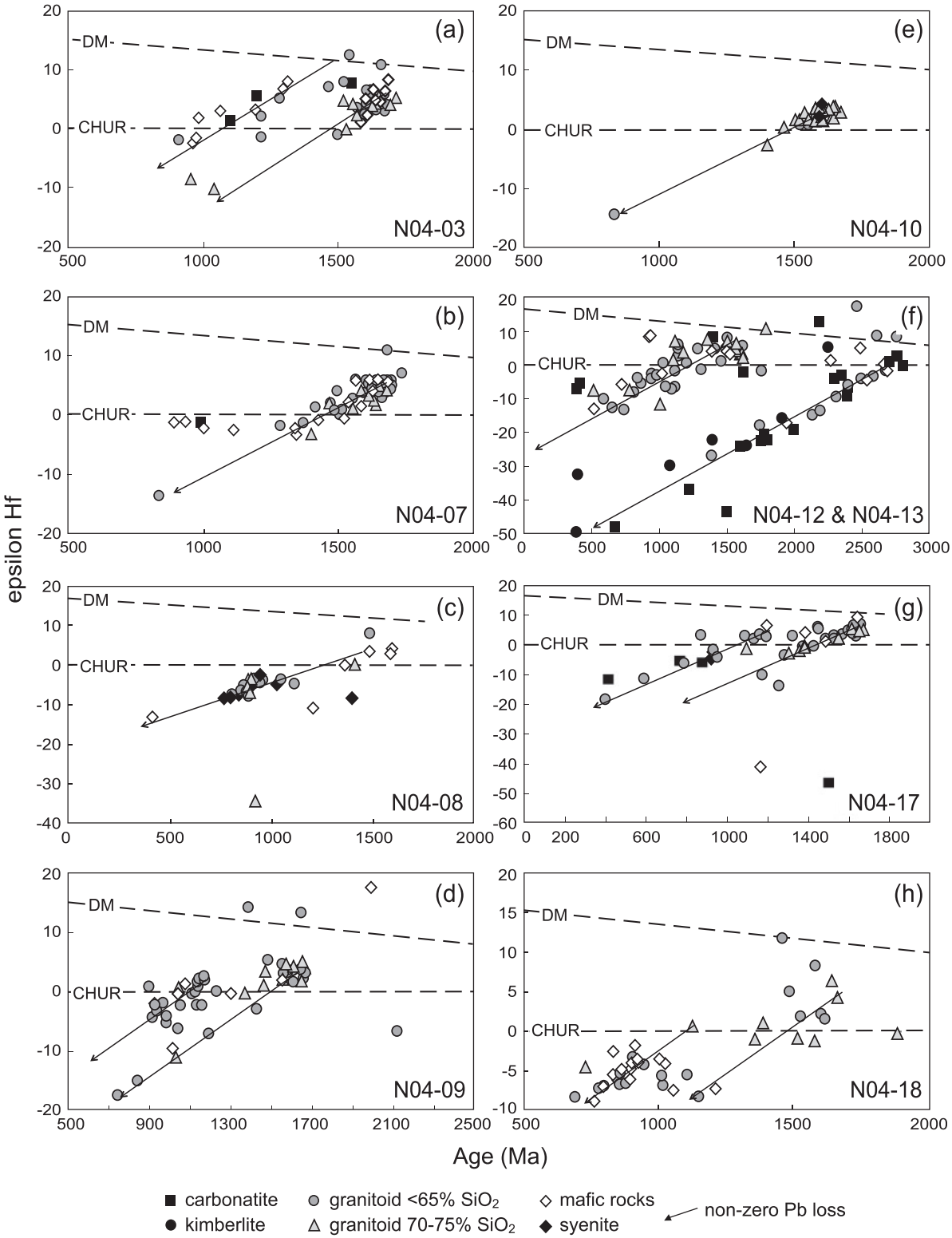

Fig. 5. Plots of εHf_t vs age for zircons from each locality. Arrows show the range in apparent εHf_t through time produced by non-zero Pb loss. Ages <1 Ga are $^{206}Pb/^{238}U$ ages; ages >1 Ga are $^{207}Pb/^{206}Pb$ ages.

non-zero Pb loss, suggesting that the real age of the population is 930–950 Ma, with $\varepsilon Hf_t = -2$ to $-4{\cdot}5$ (Fig. 5c). The older population is at least 1·58 Ga in age, with more juvenile Hf ($\varepsilon Hf_t = -5$ to $+8$). Each population contains zircons typical of a range of rock types, ranging from mafic to felsic. Two analyses of one grain with an apparent age of 916 Ma have $\varepsilon Hf_t = -34$ (not shown) and -44, corresponding to a T_{DM} of 2·7–3·0 Ga.

N04-09 (Nordfjord)

Most grains scatter along concordia (Fig. 2d), with clusters at 1·5–1·7 Ga, and 1·1–1·2 Ga and *c.* 1·0 Ga. Many of the discordant grains scatter about lines extending from *c.* 1·6 Ga toward 1·0 Ga and from *c.* 1·6 Ga toward 400 Ma; there is a weaker trend between 1·2 Ga and 400 Ma. The probability-density plot (Fig. 3d) shows a wide range of ages, with peaks in the Mesoproterozoic and Neoproterozoic. The $^{176}Hf/^{177}Hf_i$–age plot (Fig. 4d) resolves these confusing data into two distinct trails of points; one originates in a cluster at *c.* 1·63 Ga ($\varepsilon Hf_t = +1{\cdot}5$ to $+4$; Fig. 5d) and the other in a cluster at *c.* 1·2 Ga ($\varepsilon Hf_t = +2{\cdot}5$ to $-2{\cdot}5$). Both trails extend toward but do not reach Caledonian ages. The older cluster contains zircons typical of a range of granitoids, whereas the younger cluster is dominated by grains typical of low-Si granitoids and mafic rocks. One grain with a $^{207}Pb/^{206}Pb$ age of 1·6 Ga has unusually low εHf_t (-45) corresponding to a T_{DM} of 3·8 Ga. A few small peridotite bodies occur in this drainage system.

N04-10 (Stadtlandet)

Most of the grains in this sample are concordant or near-concordant, with a cluster near 1·6 Ga (Fig. 2e); only a few discordant grains scatter toward *c.* 1·0 Ga and 400 Ma. The probability-density plot (Fig. 3e) shows a major peak at 1·6 Ga. The $^{176}Hf/^{177}Hf_i$–age plot (Fig. 4e) shows a single population with a probable age of 1·64–1·67 Ga, related by non-zero Pb loss to one grain reset to *c.* 830 Ma. The sample is dominated by zircons typical of high-Si granitoids (open triangles), with $\varepsilon Hf_t = 0$ to $+4$ (Fig. 5e), and it appears likely that this represents a body of 'rapakivi granite' mapped in this drainage. No peridotite bodies are known in this Stadtlandet drainage system.

N04-12 and N04-13 (Almklovdalen)

The zircons from the drainage system that includes the large Almklovdalen peridotite complex show more complicated patterns than those in any of the other drainages. The concordant grains in these two samples occur in clusters around 2·7 Ga, 1·5–1·7 Ga and 0·9–1·1 Ga (Fig. 2f). This drainage system appears to be unique in having several concordant grains with Archean U–Pb ages. Most of the discordant grains lie inside envelopes defined by discordia lines from 2·8 to 0·4 Ga and from 1·6 to 0·4 Ga. The probability-density plot (Fig. 3f) shows a wide scatter of ages from 2·8 to 0·4 Ga with prominent peaks around 0·9, 1·5 and 1·6 Ga. However, the $^{176}Hf/^{177}Hf_i$–age plot (Fig. 4f) resolves these data into three populations with distinct Hf-isotope compositions. One extends from 2·8 Ga to 380 Ma; the second extends from 1·6 to 1·2 Ga, and possibly to 735 Ma; the third extends from 1·1–1·3 Ga to 515 Ma. These three horizontal trends reflect non-zero Pb loss from grains in each population, and imply that the real ages of all of the grains in each population are given either by the oldest ages or by their maximum model ages (up to 3·2 Ga, assuming derivation from a depleted source). The resetting of the U–Pb system in the older grains was accompanied by the local development of overgrowths (Supplementary Data, Appendix 1). Some grains in the Neoproterozoic population have Caledonian rims; grains in the Mesoproterozoic population may have rims that are either Neoproterozoic or Caledonian. In most cases these younger rims have only marginally higher $^{176}Hf/^{177}Hf$ than the cores, implying low bulk Lu/Hf and hence limited growth in $^{176}Hf/^{177}Hf$ through time in the rock that hosted the zircons. These patterns also demonstrate once again that in general, the Hf-isotope compositions of the older grains are not reset during the later events. Only two grains in the Archean population have Palaeoproterozoic rims with significantly higher $^{176}Hf/^{177}Hf$ than the cores, suggesting that the host-rock had a high bulk-rock Lu/Hf, as would be expected if it contained abundant garnet.

The oldest grains in each population have relatively juvenile Hf-isotope compositions (Fig. 5f): $\varepsilon Hf_t = 0$ to $+3$ (Archean), $+1$ to $+8$ (Mesoproterozoic) and $+1$ to $+6$ (Neoproterozoic), respectively. The large apparent negative εHf_t values of zircons with younger U–Pb ages (down to -50) are artefacts, reflecting the resetting of U–Pb ages without resetting of the Hf-isotope compositions. The T_{DM} of grains in the Archean population ranges from 2·7 to 3·2 Ga. This Archean population contains a high proportion of zircons with unusual trace-element patterns, characteristic of zircons from carbonatites (12 grains, filled squares) and kimberlites (five grains, filled circles) although some are classified as derived from low-Si granitoids (10 grains, open circles). The younger populations are dominated by zircons typical of both low-Si granitoids and high-Si granitoids (open circles and open triangles, respectively).

N04-17 (Austefjord)

About half of the grains in this sample are concordant or near-concordant, with clusters around 1·65 and 1·1 Ga (Fig. 2g); discordant grains lie near lines extending from *c.* 1·6 Ga toward 1·0 Ga and 400 Ma. The probability-density plot (Fig. 3g) shows a major peak at *c.* 1·62 Ga, and a wide scatter of ages to as young as 400 Ma. The data in the $^{176}Hf/^{177}Hf_i$–age plot (Fig. 4g) once again resolve into two major populations, one extending from 1·64–1·68 Ga ($\varepsilon Hf_t = +3$ to $+9$; Fig. 5g) to as young as *c.* 850 Ma, and

the other from 1·1–1·2 Ga ($\varepsilon Hf_t = +3$ to $+6$) to 400 Ma. Three grains with Mesoproterozoic ages have unusually low $^{176}Hf/^{177}Hf$, corresponding to εHf_t from -41 to -54, and $T_{DM} = 3{\cdot}3$–$4{\cdot}2$ Ga; these are probably Archean grains that have undergone significant non-zero Pb loss. Both the 1·64–1·68 Ga population and the 1·1–1·2 Ga population contain zircons typical of a range of felsic to mafic rocks. Peridotite bodies are known to occur in this drainage.

N04-18 (Runde)

Most of the concordant or near-concordant grains in this sample cluster around 950 Ma (Fig. 2h); the discordant grains scatter about a line between this cluster and *c.* 1·8 Ga, and a line between *c.* 950 and 400 Ma. The probability-density plot of the U–Pb ages (Fig. 3h) shows a double peak between 900 and 950 Ma and a scattering of older ages from 1·5 to 1·9 Ga. In the $^{176}Hf/^{177}Hf_i$–age plot (Fig. 4h), there is a well-defined younger cluster extending from 940–955 Ma ($\varepsilon Hf_t = -2$ to $-4{\cdot}5$; Fig. 5h) to *c.* 700 Ma. The less well-defined older population gives ages of 1·62–1·73 Ma ($\varepsilon Hf_t = -0{\cdot}5$ to $+2$) and appears to trend towards *c.* 950 Ma. The older population contains zircons typical of a range of granitoids (circles and triangles); the younger one has a high proportion of zircons typical of mafic rocks (open diamonds).

DISCUSSION

Tectonothermal history of the WGR

The combined U–Pb age spectrum for all the zircons analyzed in this study from the Western Gneiss Region is very complex (Fig. 6a), and would be misleading as a sole guide to the tectonothermal history of the region. For example, minor peaks on the spectrum could be interpreted as providing evidence for tectonothermal events between 1·7 and 1·1 Ga and between 0·9 and 0·4 Ga. However, the Hf-isotope analyses resolve these data into consistent patterns indicating two major tectonothermal events, corresponding to the Gothian (1·7–1·5 Ga) and Sveconorwegian (1·3–0·9 Ga; i.e. Grenville) orogenies (Fig. 6b and c), and successive overprinting of older populations by younger thermal events, ending with the Caledonian orogeny (*c.* 400 Ma). The oldest grains in each population can be used to constrain the age and εHf of the original magmatic event(s) (see Amelin *et al.*, 2000).

The Gothian zircon populations show a small regional variation in age, from 1·65–1·7 Ga in the northern part of the area to 1·6–1·65 Ga in the southern part; more detailed work would be required to establish whether this trend is significant. The Gothian ages are consistent with zircon ages obtained from both the northern WGR (Tucker *et al.*, 1987) and the central and southern WGR (Tucker *et al.*, 1992). The Gothian populations have mean $\varepsilon Hf_t = +2$ to $+5$, and T_{DM}^{C} model ages of 2·0–2·1 Ga. These values suggest that the magmatic rocks were derived from protoliths

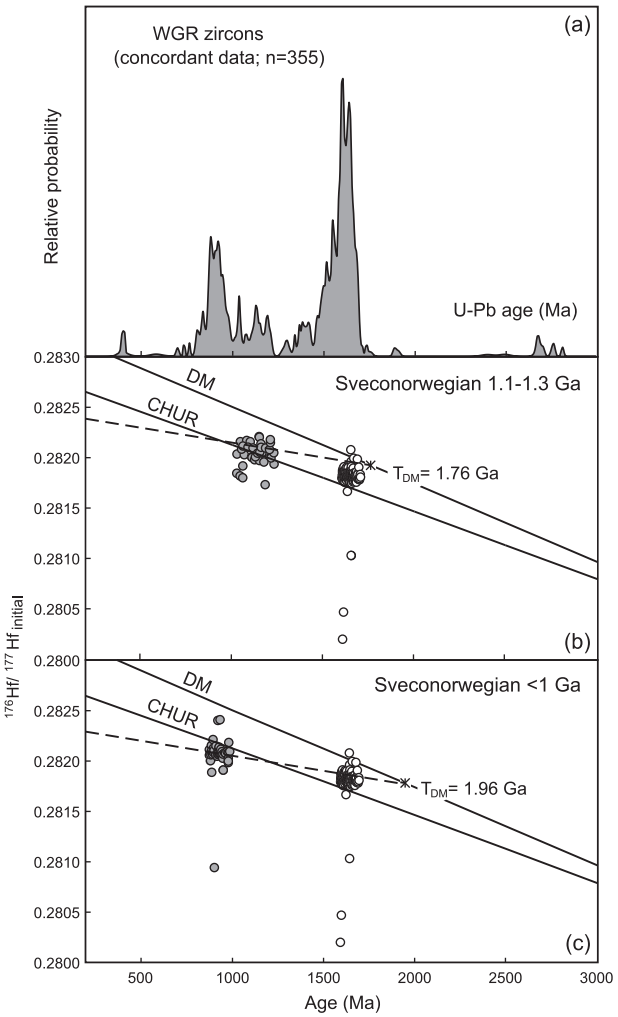

Fig. 6. (a) Composite age spectrum for all samples from the Western Gneiss Region; (b) $^{176}Hf/^{177}Hf_i$ vs U–Pb age for samples in which the Grenville population is >1·1 Ga; (c) $^{176}Hf/^{177}Hf_i$ vs age for samples in which the Grenville population is <1 Ga. Open symbols, Gothian (1·7–1·5 Ga) zircons; filled symbols, Sveconorwegian (1·3–0·9 Ma) zircons.

with a <400 Myr crustal prehistory, or represent a well-homogenized mixture of crustal and juvenile components, such as may be found in some continental-margin arc settings or in continental collisional zones where the subducted continental crust melts and mixes with the overlying mantle wedge (Brueckner, 2009).

Tucker *et al.* (1987) found no Sveconorwegian-age zircons from the northern part of the WGR (north of Storfjord). Subsequently, Tucker *et al.* (1992) obtained Sveconorwegian and Gothian ages from zircons in the central and southern portions of the WGR. Their results verified an earlier proposal (Brueckner, 1979), based on Rb–Sr isochrons, that there is a major boundary separating mixed Gothian and Sveconorwegian rocks to the south and Gothian-only

rocks to the north. Our results are generally consistent with the existence of this boundary; however, we have obtained some Sveconorwegian ages in zircons from Sundalsøra (N04-03) and Valldal (N04-07). Four Sveconorwegian-age zircons from Valldal have geochemical signatures appropriate for mafic rocks, as do several of those from Sundalsøra. These data suggest that the Gothian crust of the WGR north of Storfjord was intruded by mafic magmas, but not by voluminous granitoid melts. It is ambiguous whether or not Sveconorwegian metamorphic recrystallization reset Gothian zircons, as the Pb loss could also have occurred during the Caledonian Orogeny, as indicated by Caledonian ages on titanites from the area (Tucker *et al.*, 1987; Kylander-Clark *et al.*, 2008).

The Sveconorwegian (Grenville)-age rocks can be divided into three groups. The oldest group (Fig. 6b) gives ages of 1·1–1·2 Ga, and is relatively juvenile, with $\varepsilon Hf_t = +2$ to +6, and T_{DM}^C model ages of 1·5–2·0 Ga. The most juvenile part of this population cannot be derived from the Gothian rocks alone, if the Gothian crust was similar in composition to average continental crust; it suggests a juvenile (i.e. mantle-derived) component as well. This group has been identified in samples N04-09, -13 and -17, all from the Nordfjord–Voldsfjord area in the southern part of the area sampled (Fig. 1).

A second younger group (Fig. 6c) gives maximum U–Pb ages < 1 Ga, and has a mean $\varepsilon Hf_t < 0$. T_{DM}^C model ages for most of this group are 1·9–2·1 Ga, similar to those from the Gothian rocks, indicating that they could have been derived by simply remelting the Gothian crust. However, as in the older group, some Hf-isotope compositions suggest the presence of a juvenile component as well. This younger group of Sveconorwegian-aged rocks has been identified in samples N04-07, -8 and -18, all NE of Voldsfjord (Fig. 1).

The third group of Sveconorwegian-age zircons is found only in sample N04-03, from the Sundalsøra drainage in the NE part of the sampled area. It gives maximum ages of *c.* 1·3 Ga (Fig. 2a) and has a distinctly juvenile signature (mean $\varepsilon Hf_t = +4$, $T_{DM}^C = 1·7$ Ga). It is probable that these zircons are derived from units of the higher nappes within the Trondheim Basin drainage, some of which are of oceanic affinity and were derived outboard to Baltica (the Upper Allochthon) and others of which were derived from the westernmost fringe of Baltica (the Middle Allochthon).

Both the Gothian and the Grenville–Sveconorwegian populations show long 'tails' of younger ages at constant $^{176}Hf/^{177}Hf$ (Fig. 4), indicating Pb loss from the zircons during later thermal events, which did not affect their Hf-isotope compositions. The resetting of the Sveconorwegian populations has produced rare Scandian ages (395 Ma and 410 Ma in sample N04-17), and Scandian (*c.* 400 Ma) rims were found on both Gothian and Sveconorwegian-age zircons in samples N04-08 and N04-12. However, in most samples the lowest apparent $^{206}Pb/^{238}U$ ages in the Sveconorwegian population (as defined by the Hf isotopes) are in the range 500–700 Ma. Zircons in the Gothian populations presumably have been reset during both Sveconorwegian and Caledonian events, but few grains extend to $^{206}Pb/^{238}U$ ages <900 Ma.

The strong effect of the Sveconorwegian event on the Gothian (and Archean; see below) zircon populations, and the more limited effect of the Caledonian events on both of them, may reflect the different nature of the Sveconorwegian and Caledonian orogenies in this region. The Sveconorwegian orogeny was a high-*T*, relatively low-*P* event that produced melting within the crust (Andersen *et al.*, 2001; Andersson *et al.*, 2002; Bingen *et al.*, 2008; Brueckner, 2009). The degree of Sveconorwegian resetting of Gothian zircons is highest in the areas where the Sveconorwegian populations are older (Fig. 6b and c).

In contrast, the Caledonian event was a lower-*T*, HP to UHP metamorphic event, with limited crustal melting (Cuthbert *et al.*, 2000; Brueckner, 2009; Spengler *et al.*, 2009). It may be significant that even in samples N04-10 and N04-18, which come from the highest-*T*, *P* portion of the Caledonian UHP metamorphic gradient (Fig. 1), we found no older zircons that were completely reset to Caledonian ages, and no zircons that had grown during the Caledonian event. Across the WGR, titanites give U–Pb ages of 390–400 Ma (Tucker *et al.*, 1992, 2004; Kylander-Clark *et al.*, 2008); the temperatures of the Scandian event (700–850°C; Fig. 1) apparently were high enough to reset (or grow) titanite, but not high enough to completely reset zircon.

Waldron *et al.* (2008) presented data on detrital zircons from early Paleozoic sandstones in the Southern Uplands terrane of Scotland, which at that time lay on the eastern edge (present-day coordinates) of Laurentia (Fig. 1). The zircon age distributions are dominated by Archean material, going back to *c.* 3·6 Ga. The contrast between these populations and those reported in this work emphasizes the contrast in age and origin between the ancient Laurentian block and the juvenile Proterozoic crust of Baltica.

Zircons from Archean ultramafic–mafic complexes

Samples N04-12 and N04-13 (Almklovdalen) contain the only zircons found in this study that give concordant Archean $^{207}Pb/^{206}Pb$ ages (Figs 2f and 7a). The morphology of this population (rounded shapes, lack of internal zoning; Supplementary Data, Appendix 1) suggests that they are largely metamorphic in origin.

A wide range of $^{207}Pb/^{206}Pb$ ages at essentially constant low $^{176}Hf/^{177}Hf$ (Fig. 7b) extending from these Archean zircons suggests a single population of Archean age, which has experienced varying degrees of non-zero Pb loss. The

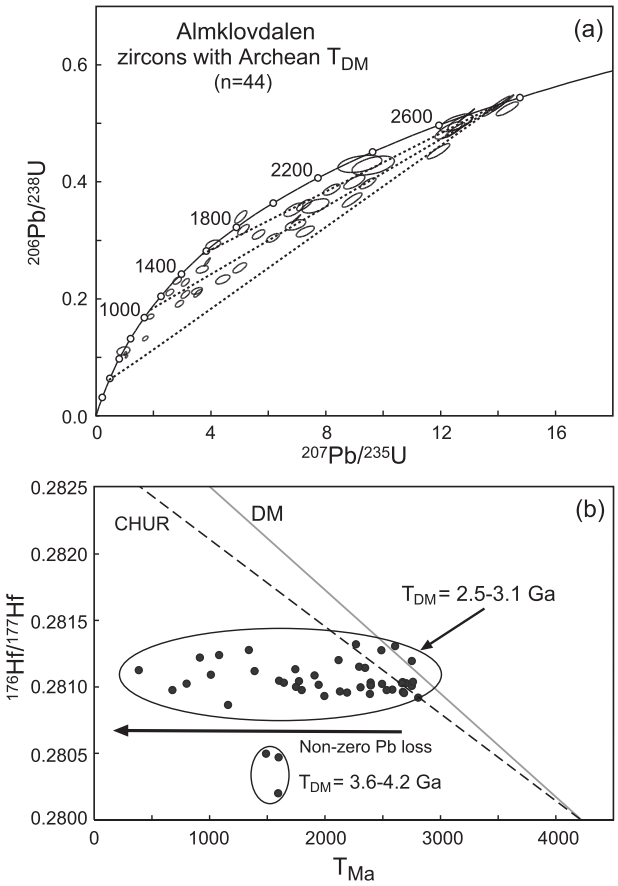

Fig. 7. (a) Concordia plot for zircons with Archean T_{DM} from Almklovdalen, showing potential discordia lines, suggesting resetting of Archean zircons during thermal events at *c.* 1·65, 1·1 and 0·4 Ga. (b) $^{176}Hf/^{177}Hf_i$ vs age, showing the effects of non-zero Pb loss from the Archean population.

pattern of discordant ages (Fig. 7a) suggests that Pb loss may have occurred during the Gothian, Sveconorwegian and Caledonian events; grains that had already lost Pb at 1·6–1·7 Ga may have been most susceptible to further loss during the Sveconorwegian and Caledonian events. However, although some grains give $^{206}Pb/^{238}U$ ages as low as 387 Ma, most grains have not equilibrated completely during the Caledonian event. This is consistent with the general scarcity of Caledonian ages in the zircons from the gneisses.

The Hf isotope compositions of these zircons can be projected back (parallel to the *x*-axis in Fig. 7b) to derive T_{DM} model ages; these range from 2·5 to 3·2 Ga [mean 2·9 ± 0·2 Ga (2σ)], close to the age of the oldest zircons in the population (2·7–2·8 Ga). These ages are consistent with Re–Os ages obtained from the Almklovdalen peridotite. Beyer *et al.* (2004) reported five whole-rock Re–Os analyses of Almklovdalen dunites with T_{MA} model ages ranging from 2·7 to 3·1 Ga. *In situ* Os-isotope analyses of single sulfide grains from garnet lherzolites gave a major peak in T_{RD} model ages in the range 2·7–3·4 Ga. They also gave a significant peak in T_{RD} model ages at 1·5–1·7 Ga, similar to the inferred age of the Gothian zircon population from samples N04-12 and N04-13.

The zircon data reported here and the Re–Os data (Beyer *et al.*, 2004) thus support one another, and both support the inference that these unusual Archean zircons were derived from the Almklovdalen ultramafic massif. This inference is consistent with their unusual trace-element chemistry, as described above. It is unlikely that these zircons would have been found by conventional whole-rock sampling, but erosion (including large-scale open-cut mining activity) and the alluvial concentration of heavy minerals has allowed the sampling of a large volume of zircon-poor ultramafic to mafic rocks.

Further support for an Archean history for the Almklovdalen peridotite masses is provided by the general tendency for peridotite clinopyroxenes and whole-rocks in the WGR to scatter around best-fit lines with Archean or early Proterozoic ages on Sm–Nd isochron diagrams (Jamtveit *et al.*, 1991; Lapen *et al.*, 2005, 2009; Spengler *et al.*, 2006; Brueckner *et al.*, 2010). Peridotite whole-rock samples and clinopyroxene separates from the northwestern WGR define a Sm–Nd best-fit line with an age of *c.* 3·2 Ga, albeit with large scatter (MSWD > 100) that is presumably the result of partial re-equilibration during subsequent events (Brueckner *et al.*, 2010).

Three zircons with Proterozoic apparent ages, but with $^{176}Hf/^{177}Hf$ similar to or lower than the Almklovdalen population, were found in sample N04-17 (T_{DM} = 3·3, 3·7, 4·1 Ga), one in sample N04-08 (T_{DM} = 2·6 Ga), and two in sample N04-09 (T_{DM} = 2·8, 3·8 Ga). Peridotite bodies occur in each of these drainages, and we suggest that these zircons also were derived from smaller ultramafic–mafic complexes, some of which may have preserved older zircons than the Almklovdalen body.

An alternative interpretation is that the Archean zircons are derived from remnant bodies of Archean trondjemite–tonalite–granite (TTG)-type gneisses, which occasionally carry zircons with the low heavy REE (HREE) contents typical of the Almklovdalen zircons. This hypothesis requires that TTG gneisses occur only in drainages that also host peridotite bodies, and that they had to contain garnet to account for the low HREE contents of many of the Archean zircons. Such gneisses have not been recognized in the Almklovdalen area, despite detailed mapping by successive generations of geologists.

Metasomatic formation of zircon in mantle peridotites

Further evidence of a derivation from the peridotites is given by the trace-element patterns of zircons with Archean T_{DM} ages from samples N04-12 and N04-13, summarized in Fig. 8. These are grouped according to their

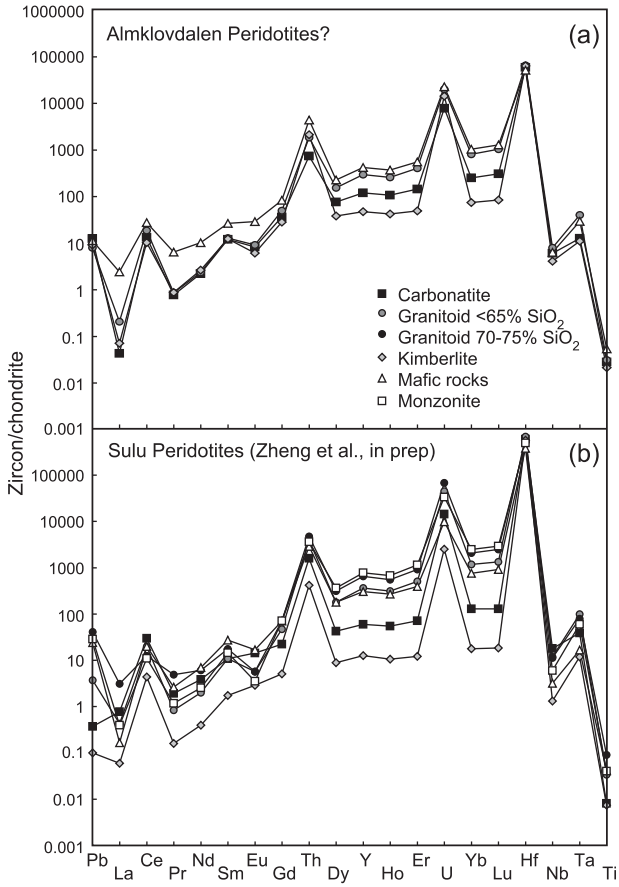

Fig. 8. (a) Chondrite-normalized trace-element patterns of zircons with Archean T_{DM} from Almklovdalen; (b) chondrite-normalized trace-element patterns of zircons from peridotites of the Sulu UHP terrane, eastern China (Zheng *et al.*, in preparation).

classification using the 'short tree' of Belousova *et al.* (2002). They show a wide range of patterns, most with pronounced positive Ce anomalies and some with small negative Eu anomalies. Those with low HREE classify largely as derived from ultramafic rocks (i.e. kimberlites, carbonatites), and those with higher HREE contents and HREE/LREE (light REE) classify as derived from low-Si granitoids or mafic rocks.

However, this classification scheme was designed only for application to magmatic zircons, whereas these Archean zircons are almost certainly metasomatic or metamorphic, based on their morphology. The classifications can only be taken as emphasizing their unusual trace-element characteristics. For example, those zircons classifying as kimberlitic do so because of low contents of Lu (<2·7 ppm) and Hf>0·62%, but their relatively high U and Y contents (Table 3) distinguish them from typical kimberlitic zircons. Similarly, many of the 'carbonatitic' zircons have higher Y, U or Hf contents than carbonatite zircons analyzed by Belousova *et al.* (2002).

The low HREE contents of many of the zircons may reflect derivation from garnet-bearing rocks, in which HREE are sequestered into garnet rather than zircon. Garnet peridotites and pyroxenites as well as internal eclogites are well known within the Almklovdalen body (Eskola, 1921; Medaris, 1980; Medaris & Carswell, 1990; Brueckner *et al.*, 2010), and reflect the refertilization of the dominant, primary garnet-free dunites and harzburgites (Beyer *et al.*, 2006; Griffin *et al.*, 2008; references therein). Zircon grains with higher HREE/LREE may be derived from the dominant garnet-free rocks, including the dunites. Beyer *et al.* (2006) argued, on the basis of Proterozoic Re–Os model ages for sulfide grains in some garnet lherzolites, that the refertilization of the dunites was a Proterozoic event. However, the zircon data presented here require another refertilization event already in Archean time (2·8–2·9 Ga), not long after the original depletion event (>3·0 Ga).

The presence of metasomatic zircon in ultramafic rocks has been documented previously, both from mantle-derived peridotite xenoliths (Zheng *et al.*, 2006*a*, 2008; Zhang *et al.*, 2007; references therein) and from 'orogenic' peridotite massifs and their enclosed eclogites in UHP terranes (Zheng *et al.*, 2006*b*, in preparation; Zhang *et al.*, 2009; references therein). In most reported instances, the peridotitic zircons show distinct age populations related to events in the overlying crust, and a range of trace-element patterns reflecting the compositions of metasomatic fluids that introduced Zr into previously depleted rocks.

Figure 8b shows the range of compositions observed by Zheng *et al.* (in preparation) in zircons extracted from peridotitic rocks of the Sulu UHP belt of eastern China. These zircons show patterns that are similar to those of the Almklovdalen zircons, but span an even larger range of REE–U–Th contents, HREE/LREE and negative Eu anomalies than the Almklovdalen zircons. Based on these geochemical arguments and the fact that no Archean zircons have been found in drainage systems that lack peridotite bodies, we conclude that the Almklovdalen zircons with Archean T_{DM} ages are derived from the peridotites and associated mafic rocks.

Where do the peridotites come from?

The data presented here indicate that the Gothian crust of southern Baltica is largely juvenile in origin. When the data are corrected for the Pb loss that occurred during the later Sveconorwegian and Scandian events, the mean εHf_t of the 1·6–1·7 Ga zircons is ≈7 (equivalent to a mean $^{176}Hf/^{177}Hf_i$ value for this population of 0·28185; Fig. 6b). This high value argues against the involvement of any pre-existing Archean components in the genesis of the gneisses. The suggestion by Lapen *et al.* (2005) that the Archean heritage of the gneisses has been obscured or erased by later events therefore seems unlikely.

Table 3: Trace elements in zircon from samples N04-12 and N04-13

Sample:	N04-12-02	N04-12-05	N04-12-12	N04-12-14C	N04-12-14R	N04-12-16	N04-12-17C	N04-12-17R	N04-12-19C	N04-12-19R	N04-12-22C
Hf T_{DM}:*	1·60	1·65	1·92	1·23	1·29	1·74	1·87	1·80	1·90	1·63	2·69
Ti	27·29	10·75	7·41	7·26	<1·51	672·6	3·72	4·83	28·38	86·32	94·18
Y	640·05	1077·69	487·3	1277·18	110·99	1510·22	1366·46	1008·98	1963·85	414·91	959·61
Nb	2·61	1·501	1·073	5·24	2·74	15·68	2·59	1·437	3·32	2·5	1·545
La	0·489	0·185	0·0152	<0·0182	0·0984	1·193	0·027	0·0198	0·376	7·64	0·258
Ce	6·88	29·65	10·56	50·86	9·31	91·1	32·4	29·15	31·31	46·95	20·11
Pr	0·205	1·068	0·0337	0·097	0·0341	0·832	0·1411	0·123	0·338	4·89	0·383
Nd	1·876	13·49	0·709	1·521	0·138	5·64	2·7	2·127	2·76	30·84	5·5
Sm	2·76	14·28	1·551	4·12	0·244	6·59	5·36	4·45	3·69	12·12	6·95
Eu	0·231	4·01	0·579	0·453	0·0793	1·112	1·338	1·22	0·611	2·95	2·37
Gd	14·69	43·73	9·33	22·89	1·813	29·43	26·54	22·76	20·89	15·83	25·6
Tb	4·82	11·77	3·08	8·04	0·706	10·24	9·04	7·44	9·09	2·459	7·11
Dy	60·63	123·66	41·27	109·92	9·19	132·84	117·97	93·78	139·04	29·39	81·09
Ho	22·53	39·25	16·39	42·96	2·9	50·3	46·91	35·53	59·9	12·24	29·91
Er	100·05	154·92	79·91	210·05	12·89	236·44	225·25	164·49	322·69	70·23	142·18
Tm	20·5	30·36	17·81	46·53	2·712	51·52	50·2	35·54	84·32	20·52	33·73
Yb	183·2	256·02	171·35	446·92	23·95	469·53	476·33	329·87	933·63	247·24	342·94
Lu	33·94	44·33	36·32	89·42	4·82	90·9	94·06	65·48	196·25	59·9	69·15
Hf	11023·7	9327·8	10175·7	16111·6	16111·6	11871·7	11871·7	11871·7	15263·6	15263·6	9327·8
Ta	1·134	0·843	0·561	2·217	1·489	3·96	0·817	0·487	4·84	4·08	0·489
Pb	86·85	41·3	88·83	272·56	176·34	295·64	129·55	98·71	2150·34	670·85	421·9
Th	68·77	106·24	46·23	208·68	22·94	793·22	94·49	83·63	365·41	39·81	243·13
U	117·45	123·02	176·07	295·93	761·07	729·67	163·08	109·02	2357·47	1012·89	273·19

Sample:	N04-12-22R	N04-12-32	N04-12-44	N04-12-45C	N04-12-45R	N04-12-48	N04-12-49	N04-12-57C	N04-12-64	N04-12-66C	N04-12-66R
Hf T_{DM}:	2·63	2·29	1·60	1·40	1·24	1·59	1·47	1·63	1·90	1·17	1·16
Ti	3·8	8·9	9·1	3·7	3·6	20·3	8·7	9·1	22·3	28·1	3·3
Y	181	597	1184	1253	176	2789	1619	1175	444	2144	556
Nb	0·51	1·63	3·78	20·64	4·12	12·64	3·34	4·14	4·07	25·06	3·81
La	0·0484	0·22	0·1602	0·1262	<0·0058	1·436	3·27	0·0366	9·27	8·17	0·0186
Ce	5·69	7·9	77·97	16·93	1·95	32·52	26·16	60·15	35·68	67·52	7·69
Pr	0·017	0·0722	0·791	0·1881	0·0073	1·636	1·362	0·378	4·44	4·82	0·0276
Nd	0·232	0·628	11	2·53	0·049	15·77	9·55	6·5	21·76	28·71	0·64
Sm	0·536	1·54	13·3	4·46	0·445	14·05	5·16	10·08	4·94	11·38	1·643
Eu	0·212	0·102	2·94	0·433	0·228	4·34	1·199	2·32	0·964	5·52	0·0528
Gd	2·95	8·99	43·11	24·68	3·7	54·35	23·57	39·06	7·79	44·35	10·63
Tb	0·969	3·24	11·59	8·78	1·437	18·73	8·45	11·2	2·19	14·45	3·8
Dy	12·88	46·29	124·51	115·37	17·46	247·79	116·89	123·64	30·14	194·43	50·94
Ho	5·35	18·96	40·93	43·57	5·71	96·03	48·73	41·11	13·51	74·51	19·01
Er	27·84	97·63	171·9	200·73	23·14	463·89	256·2	172·56	76·1	332·69	87·54
Tm	7·11	21·79	35·58	43·65	4·59	103·78	64·21	35·53	19·73	65·88	17·95
Yb	78·85	209·73	323·47	398·59	41·76	970·81	685·06	320·68	220·19	557·45	163·52
Lu	17·23	42·87	57·05	69·92	7·48	168·81	141·45	55·57	49·55	95·76	30·02
Hf	9328	12720	11024	13568	13568	11872	15264	14416	12720	9328	9328
Ta	0·303	1·203	1·018	8·86	1·503	5·03	5·67	1·435	2·55	6·63	1·313
Pb	109·35	307·85	96·19	141·03	41·74	804·29	4008·28	46·27	374·77	442·46	84·55
Th	66·13	106·27	208·48	51·3	2·75	607·2	750·93	140·73	97·32	419·73	66·86
U	114·56	246·52	155·14	253·71	163·71	1006·71	5764·82	78·25	436·75	774·81	153·88

(continued)

Table 3: Continued

Sample:	N04-12-67	N04-12-69	N04-12-70C	N04-12-70R	N04-12-72	N04-12-73	N04-12-75	N04-12-77C	N04-12-77R	N04-12-78	N04-12-83
Hf T_{DM}:	1·86	1·78	1·86	1·86	1·58	1·88	1·85	1·98	1·97	2·26	1·74
Ti	118·4	4·6	12·0	10·0	7·9	17·3	5·6	14·1	6·4	42·4	22·6
Y	1108	545	1363	556	2094	1517	1406	2242	1078	29	679
Nb	7·31	1·69	1·08	0·95	3·27	4·65	3·14	3·38	7·43	0·33	3·06
La	3·41	<0·0067	0·0294	0·0123	0·0613	0·74	0·0181	0·0155	<0·0103	0·0259	0·095
Ce	25·39	9·51	19·65	12·95	43·35	45·33	8·35	46·4	41·27	2·00	11·59
Pr	1·064	0·0242	0·414	0·0661	0·399	0·461	0·0304	0·341	0·0527	0·022	0·1193
Nd	5·43	0·598	6·3	0·97	6·57	4·53	0·612	5·79	0·948	0·225	1·372
Sm	3·53	1·403	7·21	1·735	10·78	6·11	1·871	11·29	2·35	0·405	2·22
Eu	0·348	0·1208	2·084	0·676	3·12	1·694	0·333	1·499	0·329	0·246	0·424
Gd	16·48	8·85	29·03	9·35	52·54	31·63	14·98	56·61	14·84	1·83	12·29
Tb	5·77	3·19	9·15	3·13	15·86	10·35	6·49	17·23	5·72	0·397	4·4
Dy	84·15	45·08	114·25	42·5	196·44	135·49	103·76	214·48	83·67	3·29	58·92
Ho	35·6	17·86	43·68	17·25	71·75	51·24	45·89	76·15	34·73	0·852	23·59
Er	182·4	87·64	207·93	89·18	321·89	236·21	248·8	341·23	177·91	3·1	111·13
Tm	41·79	19·27	46·7	21·88	68·25	50·88	60·98	71·67	42·83	0·657	24·04
Yb	412·29	184·56	455·7	238·33	632·32	477·08	625·33	652·84	435·22	6·6	228·63
Lu	82·4	35·85	88·18	51·81	113·08	88	123·47	116·41	85·37	1·568	45·75
Hf	13568	11024	11024	11024	12720	11872	12720	12720	12720	10176	14416
Ta	3·63	0·701	0·473	0·43	1·17	1·643	1·8	1·677	3·46	0·086	1·279
Pb	373·76	79·55	66·24	66·26	263·4	202·82	225·06	272·53	307·93	83·85	148·42
Th	256·41	34·96	53·32	40·21	251·31	200·52	57·74	296·58	204·56	15·27	84·57
U	499	80·79	63·07	61·92	393·45	200·95	223·94	239·31	325·3	408·43	372·03

Sample:	N04-12-84	N04-12-92	N04-12-97	N04-12-98	N04-12-105	N04-12-116	N04-12-119	N04-12-122	N04-12-124C	N04-12-124R	N04-12-140C
Hf T_{DM}:	2·89	2·46	1·85	3·12	1·92	1·88	2·05	3·02	2·65	2·12	2·80
Ti	1·8	10·2	6·4	42·8	12·2	20·2	10·6	3·6	12·4	5·0	7·4
Y	16	399	879	675	1410	1276	2006	2781	1017	246	601
Nb	0·23	1·41	4·06	3·81	7·81	2·80	3·18	4·55	1·17	1·22	1·67
La	<0·0060	0·0229	0·033	0·546	0·0095	0·0269	0·0894	0·1253	0·0127	0·0075	<0·0052
Ce	1·144	22·23	21·29	20·74	46·98	28·29	17·6	12·89	8·13	6·8	7·15
Pr	<0·0046	0·206	0·0786	0·454	0·0613	0·1222	0·1212	0·354	0·0673	0·036	0·0176
Nd	0·051	3·67	1·17	3·08	1·537	2·25	1·59	5·33	1·36	0·797	0·476
Sm	0·215	6·75	2·38	2·01	3·71	4·12	4·14	9·97	3·17	1·462	1·119
Eu	0·381	0·979	0·186	2·62	0·448	1·063	0·576	1·107	1·064	0·312	0·258
Gd	1·584	23·12	14·31	10·43	22·64	23·48	25·05	59·22	21·86	5·78	8·61
Tb	0·353	5·39	5·4	3·73	8·42	8·17	10·6	19·96	7·21	1·658	3·19
Dy	2·45	49·77	75·45	52·76	118·09	108·03	157·83	257·56	87·88	18·71	44·48
Ho	0·507	14·3	30·66	21·58	47·9	43·35	67·73	98·61	32·97	7·58	18·47
Er	1·498	54·17	147·33	106·45	234·16	207·5	341·84	425·45	150·24	40·26	93·02
Tm	0·2211	10·65	32·85	24·67	54·88	45·66	81·24	82·58	32·7	10·19	22·01
Yb	1·912	92·65	309·64	243·93	544·51	434·64	803·02	690·96	315·5	109·86	228·24
Lu	0·303	16·57	58·18	47·86	100·31	83·99	154·28	120·07	61·73	23·65	47·47
Hf	10176	13568	8480	13568	13568	11024	12720	10176	10176	10176	13568
Ta	0·0626	0·769	1·192	3·12	3·7	0·99	1·423	2·151	0·439	0·395	1·505
Pb	10·99	324·95	95·56	1056·64	417·87	162·28	206·04	910·94	231·96	111·07	520·81
Th	0·66	427·64	54·88	211·69	294·6	154·43	106·78	310·45	79·93	26·91	89·47
U	50·64	284·81	107·33	1321·21	443·92	170·79	203·21	497·94	177·53	96·97	312·76

(continued)

Table 3: Continued

Sample:	N04-12-140R	N04-12-147	N04-12-148	N04-12-173	N04-12-176	N04-12-196	N04-12-206	N04-13-01	N04-13-02	N04-13-03	N04-13-04
Hf T_{DM}:	2·80	1·84	3·00	1·78	1·61	3·09	1·86	3·00	2·85	1·61	3·02
Ti	6·6	24·0	6·2	11·4	11·7	79·4	3·4	13·5	19·0	11·9	28·2
Y	638	1036	253	1784	622	856	1359	338	153	459	215
Nb	1·24	3·56	0·29	8·51	1·75	2·54	2·37	3·38	2·65	4·08	2·43
La	<0·0091	0·0041	<0·0055	3·42	0·014	4·83	0·0159	0·02	<0·0126	<0·0119	0·03
Ce	5·76	17·45	9	92·44	41·04	51·04	31·24	11·1	12·23	18·41	8·6
Pr	0·0435	0·0504	0·0355	3·96	0·225	4·22	0·1803	0·1474	0·0817	0·0425	0·152
Nd	0·712	1·025	0·571	26·46	3·84	27·32	3·59	2·141	1·357	0·821	2·33
Sm	1·77	2·607	1·166	14·26	5·44	11·88	6·47	3·14	2·06	1·659	5·2
Eu	0·49	0·258	0·547	2·008	1·448	8·71	2·061	1·066	0·56	0·299	1·636
Gd	12·29	16·68	6·06	37·62	20·85	35·8	31·04	12·33	7·05	9·01	18·84
Tb	4·07	6·26	1·89	11·43	5·68	8·44	9·54	3·4	1·667	3·08	3·68
Dy	50·87	85·76	22·25	144·23	62·01	83·52	119·34	36·18	16·9	40·93	30·14
Ho	20·18	34·29	7·91	56·45	21·02	25·11	45·71	11·48	5·23	15·81	7·52
Er	97·02	163·07	36·16	269·93	89·34	97·76	211·07	46·49	21·01	75	24·17
Tm	22·11	36·46	8·33	61·82	18·48	19·3	46·38	9·21	4·14	16·68	4·32
Yb	216·28	347·13	79·09	592·64	167·86	175·26	444·37	82·55	37·43	162·92	33·24
Lu	45·96	63·47	14·78	109·83	30·58	34·82	83·3	14·34	6·56	31·17	5·19
Hf	13568	11872	11024	11872	11024	10176	9328	8310	9837	8480	8650
Ta	0·67	1·374	0·0661	2·316	0·604	0·778	0·655	0·365	0·0927	0·61	0·225
Pb	207·46	169·15	15·71	571·52	35·3	744·86	88·77	22·96	108·83	25·14	511
Th	61·6	90·37	8·82	559·92	64·9	333·44	104·38	7·17	35·82	26·59	71·59
U	242·5	180·2	21·07	734·15	54·43	599·05	164·07	20·78	64·39	31·7	237·06

Sample:	N04-13-05	N04-13-06	N04-13-07	N04-13-08	N04-13-09	N4-13-10	N4-13-11	N4-13-12	N4-13-13	N4-13-14	N4-13-15
Hf T_{DM}:	1·44	1·74	3·05	3·01	2·90	1·69	1·44	1·88	1·87	3·11	2·94
Ti	13·7	19·3	12·6	14·8	31·7	19·5	10·6	17·5	15·2	54·9	9·7
Y	1097	686	443	63	99	508	833	755	923	1455	129
Nb	4·19	4·39	2·65	2·24	3·11	4·17	12·05	7·42	3·98	6·09	2·25
La	0·04	0·03	0·02	0·03	<0·0174	<0·0156	<0·0115	0·09	<0·031	0·14	<0·0159
Ce	6·73	2·565	28·84	18·46	0·97	16·74	16	20·96	24·86	40·13	11·06
Pr	0·345	0·127	0·176	0·365	<0·0176	0·0598	0·0278	0·084	<0·029	0·285	0·0657
Nd	4·97	2·22	2·85	5·5	0·142	0·788	0·558	1·08	0·938	4·94	1·412
Sm	7·34	4·02	4·1	4·97	0·534	1·81	1·793	1·88	1·794	8·62	3·33
Eu	0·629	1·095	1·528	0·801	0·411	0·284	0·177	0·14	0·541	1·955	0·278
Gd	29·98	18·66	15·55	8·46	3·26	9·08	11·01	9·2	11	42·11	10·45
Tb	9·79	5·7	3·94	1·476	0·987	3·29	4·59	3·55	4·26	12·26	2·057
Dy	118·41	68·3	42·78	10·35	10·61	43·48	66·87	53·08	63·66	141·72	16·54
Ho	41·11	24·02	14·91	2·077	3·14	17·17	28·06	23·91	27·56	50·35	4·33
Er	174·19	103·34	64·79	5·86	11·46	83·6	141·55	127·65	147·87	213·95	14·66
Tm	35·19	20·77	13·51	0·87	2·111	18·92	31·56	31·21	36·19	41·13	2·552
Yb	319·31	189·18	129·27	6·51	18·92	182·88	294·35	331·25	386·86	354·32	20·49
Lu	58·61	35·52	26·04	0·926	3·3	36·22	52·13	69·94	84·02	67·39	3·61
Hf	6954	12126	7971	10261	11533	10091	10346	13144	10854	8310	13059
Ta	0·629	0·509	0·295	0·163	0·5	0·808	4·08	2·9	1·236	1·251	0·331
Pb	48·91	56·63	81·83	95·93	221·99	32·46	70·04	433·14	692·24	519·8	102·48
Th	58·16	11·05	107·23	116·24	4·6	32·24	36·3	124·26	280·06	184·1	71·45
U	67·12	67·73	95·07	75·62	198·89	51·7	128·96	374·29	615·04	255·99	79·14

(continued)

Table 3: Continued

Sample:	N4-13-16	N4-13-17	N4-13-18	N4-13-19	N4-13-22	N4-13-23	N4-13-24	N4-13-25	N4-13-27	N4-13-29	N4-13-30
Hf T_{DM}:	1·50	2·91	1·91	1·73	1·68	1·55	3·01	3·01	1·72	1·65	1·53
Ti	13·5	11·1	16·1	176·9	10·5	8·6	16·4	16·6	15·4	10·9	11·5
Y	1658	383	2079	1154	858	668	68	723	662	905	415
Nb	4·10	2·76	4·24	9·69	7·13	2·51	1·78	2·78	5·03	12·45	2·43
La	0·07	<0·0165	0·10	0·96	0·03	<0·0169	0·12	<0·0176	<0·0149	<0·022	<0·0173
Ce	8·36	17·19	45·32	15·38	32·42	5·85	5·24	17·19	16·06	32·46	4·12
Pr	0·807	0·0873	0·337	0·774	0·031	0·0528	0·147	0·127	0·0362	0·087	0·0433
Nd	13·12	1·462	5·49	5·8	0·92	1·117	1·547	2·56	0·73	1·046	0·687
Sm	16·79	2·3	8·71	5·17	2·58	2·45	3·31	5·22	2·72	2·18	1·64
Eu	0·956	0·386	3·99	1·39	0·371	0·342	0·677	1·763	0·839	0·234	0·125
Gd	59·39	9·75	41·61	22·67	13·2	13·83	11·91	23·55	16·37	11·34	8·18
Tb	16·36	2·953	12·9	7·6	5·08	4·69	2·233	6·62	5·19	4·6	2·9
Dy	180·3	34·49	162·56	97·97	69·9	60·06	12·89	74·41	62·39	67·57	36·95
Ho	60·76	12·54	64·46	38·41	27·35	22·56	2·115	24·97	21·91	28·46	13·99
Er	251·99	57·38	313·02	181	135·77	102·83	5·02	103·41	95·96	153·05	65·27
Tm	49·54	12·52	71·73	38·75	30·86	21·44	0·651	20·22	19·51	38·11	13·93
Yb	444·13	118·56	730·22	365·41	300·23	198·6	4·64	179·45	177·19	381·7	132·63
Lu	85·69	23·52	154·57	69·17	60·06	39·21	0·637	34·17	33·5	71·3	25·25
Hf	10430	12126	8310	13313	12550	7886	12720	9921	12211	13398	8734
Ta	0·543	0·567	0·807	2·67	2·506	0·429	0·332	0·484	1·145	6·32	0·471
Pb	44·5	38	409·97	469·15	51·87	20·54	828·91	42·38	263·46	67·16	29·71
Th	43·97	34·87	331·17	133·61	104·29	24·28	30·02	24·3	125·37	128·64	13·45
U	61·01	40·09	349·18	483·31	97·47	37·35	437·01	22·66	428·76	92·52	33·84

Sample:	N4-13-31	N4-13-32	N4-13-33	N4-13-34	N4-13-35	N4-13-36	N4-13-37	N4-13-38	N4-13-40	N4-13-43	N4-13-44
Hf T_{DM}:	1·69	1·89	1·71	3·04	3·06	1·74	1·71	1·56	3·09	1·83	1·58
Ti	11·2	14·1	458·9	8·6	45·4	50·8	9·4	32·8	20·7	11·7	17·5
Y	505	854	974	55	296	440	519	1965	457	594	531
Nb	4·34	2·18	8·23	1·46	2·26	1·81	6·47	3·45	2·03	3·31	3·68
La	<0·0144	<0·0176	0·05	0·04	<0·0183	0·58	0·01	0·14	0·03	<0·0123	<0·066
Ce	23·37	15·11	9·55	6·71	15·48	7·83	26·43	39·93	16·49	8·58	6·77
Pr	0·0541	0·1	0·257	0·132	0·1	0·121	0·052	1·085	0·133	0·0431	<0·049
Nd	0·964	1·81	4·07	2·26	1·261	1·04	0·798	13·88	2·23	0·705	0·696
Sm	1·78	3·46	6·53	2·87	1·92	1·63	1·759	17·42	3·87	1·728	1·78
Eu	0·221	0·754	2·554	0·383	0·709	0·501	0·167	6·04	0·623	0·309	0·205
Gd	9·4	17·09	27·25	6·83	9·06	7·87	7·87	75·19	16·32	10·11	9·63
Tb	3·32	5·69	7·92	1·209	2·517	2·64	3·01	20·32	4·34	3·61	3·43
Dy	42·92	71·04	90·45	8·58	28·31	34·65	41·76	217·36	46·11	48·89	45·22
Ho	16·79	27·86	31·22	1·789	9·77	14·86	17·01	69·48	15·34	19·61	17·64
Er	81·95	132·06	138·5	5·43	42·87	68·91	86·72	274·61	62·37	93·86	84·13
Tm	18·58	28·54	29·36	0·869	8·67	16·34	20·87	52·3	11·67	20·39	18·31
Yb	177·83	273·01	284·72	6·27	80·84	161·65	213·68	446·05	103·04	197·53	175·68
Lu	34·86	53·43	54·59	0·965	15·22	32·57	41·3	79	19·72	39·4	34·25
Hf	9498	8904	6530	11024	9752	7462	10685	9752	12126	9328	8904
Ta	1·029	0·436	1·737	0·0664	0·275	0·494	2·289	0·789	0·234	0·879	0·731
Pb	44·15	108·36	37·76	195·69	20·62	138·5	24·74	85·09	6·54	91·48	31·21
Th	52·32	78·93	23·61	119·61	14·2	41·87	56·71	316·05	1·125	38·66	24·79
U	76·04	95·12	60·92	128·04	21·88	137·68	31	134·06	10·9	110·64	57·48

(continued)

Table 3: Continued

Sample:	N4-13-45	N4-13-46	N4-13-47	N4-13-48	N4-13-53	N4-13-54	N4-13-55	N4-13-56	N4-13-58	N4-13-59	N4-13-61
Hf T_{DM}:	1·51	3·11	3·15	3·06	3·12	3·04	1·84	1·91	2·87	2·17	3·10
Ti	54·3	8·8	16·1	15·0	17·1	18·9	11·6	17·4	18·2	8·6	11·5
Y	645	395	310	363	426	358	825	995	170	106	316
Nb	5·98	2·75	2·24	2·11	2·46	1·81	3·79	5·06	1·52	1·93	2·36
La	<0·0094	<0·0151	<0·0192	0·04	0·01	<0·0175	0·02	<0·0162	0·04	0·02	0·02
Ce	26·88	30·98	19·81	17·07	39·37	22·12	22·06	39·48	1·295	6·85	15·63
Pr	0·05	0·0513	0·1215	0·1264	0·1348	0·14	0·09	0·098	0·0362	0·0306	0·112
Nd	0·807	1·003	1·592	1·908	2·145	2·112	1·31	1·91	0·689	0·556	1·739
Sm	1·83	2·032	2·52	2·74	3·45	3·06	2·36	3·57	2·54	0·917	2·99
Eu	0·242	0·517	0·338	0·662	1·17	0·708	0·271	0·809	0·169	0·616	0·917
Gd	10·66	9·35	10·22	12·29	13·87	11·94	15·69	19·16	13·73	4·5	11·18
Tb	3·8	2·809	2·801	3·14	3·75	3·25	5·53	6·31	3·46	1·213	3·11
Dy	52·72	34·31	30·67	34·66	42·05	35·09	70·72	83·18	24·99	12·23	33·29
Ho	21·15	12·72	10·41	12·03	14·66	11·86	27·63	32·7	5·14	3·68	11·06
Er	105·32	60·29	44·53	51·78	63·82	49·7	130·34	159·69	14·43	12·66	45·95
Tm	24·31	13·27	9·13	10·19	12·91	9·95	28·59	36·08	2·165	2·159	9·23
Yb	244·15	130·41	84·29	96·82	118·3	90·12	269·96	360·05	15·9	16·39	81·66
Lu	48·57	25·6	16·52	19·95	23·72	17·3	51·45	72·22	2·143	2·464	14·8
Hf	9837	8904	11872	11618	7632	9752	12974	12805	13653	8650	9922
Ta	1·535	0·815	0·28	0·192	0·562	0·214	1·263	1·377	0·314	0·569	0·359
Pb	106·44	150·71	14·43	15·67	144·2	37·93	84·76	120·66	1223·09	127·24	3·01
Th	72·54	62·17	1·313	3·43	50·21	49·35	44·41	96·97	43·34	57·04	0·371
U	130·43	114·31	12·97	17·33	67·6	18·32	90·74	153·38	696·8	108·77	5·53

Sample:	N4-13-65	N4-13-70	N4-13-71	N4-13-72	N4-13-73	N4-13-74	N4-13-76	N4-13-80	N4-13-82	N4-13-83	N4-13-86
Hf T_{DM}:	1·65	2·74	3·04	3·13	3·04	1·71	2·94	3·08	2·69	3·16	3·03
Ti	25·1	10·9	15·9	7·6	18·0	22·4	13·7	16·7	10·8	26·8	12·1
Y	1923	129	341	232	358	876	101	491	69	301	721
Nb	4·05	2·14	3·03	2·06	3·25	5·34	1·71	3·47	1·96	3·19	3·81
La	0·20	<0·0176	0·02	<0·0100	0·01	0·10	0·08	<0·0128	<0·0107	<0·0155	<0·0107
Ce	51·69	14·02	19·59	13·54	12·41	31·71	11·06	26·81	7·37	7·74	27·49
Pr	1·212	0·0804	0·1051	0·087	0·1447	0·181	0·1044	0·1363	0·0601	0·0738	0·0719
Nd	16·31	1·209	1·394	1·195	2·055	2·62	1·155	2·455	1·057	1·566	1·082
Sm	21·15	1·88	3·08	1·93	3·02	4·67	1·456	4·34	2·014	3·68	2·8
Eu	6·73	0·731	0·502	0·658	1·121	0·398	0·744	0·375	0·285	0·693	0·364
Gd	83·3	7·6	13·86	7·2	11·84	22·87	4·76	17·78	6·01	13·85	15·77
Tb	20·91	1·764	3·88	1·937	3·45	7·01	1·078	4·92	1·315	3·67	5·11
Dy	213·42	15·92	39·58	21·9	38	85·05	10·35	52·17	10·38	35·8	64·41
Ho	67·7	4·15	11·66	7·71	12·5	31·45	3·23	17·29	2·339	10·37	24·28
Er	264·9	13·76	40·99	33·62	51·71	140·91	14·17	69·72	7·1	37·76	110·58
Tm	50·6	2·245	6·77	7·13	10·07	28·83	3·2	13·64	1·112	6·82	23·29
Yb	432·24	17·9	50·56	68·51	88·55	264·57	32·94	122·91	8·39	56·98	215·02
Lu	77·05	2·74	8·58	14·12	17·38	53·68	7·14	24·01	1·364	9·79	41·17
Hf	7547	10685	10685	8904	10006	14331	7462	13483	10770	16366	9582
Ta	0·83	0·539	0·572	0·401	0·536	0·817	0·1382	0·946	0·228	0·858	0·875
Pb	63·03	28·93	93·56	148·24	17·14	26·35	35·11	182·66	38·1	183·57	101·42
Th	265·3	13·1	84·16	52	4·16	34·97	35·1	49·31	16·5	30·39	69·85
U	100·21	46·82	75·42	92·04	20·58	31·15	51·8	105·71	43·09	82·21	53·1

*Hf T_{DM} values are reported to distinguish zircons with Archean Hf model ages.

The peridotites and their associated rocks, on the other hand, are clearly Archean; the U–Pb ages and Hf-isotope model ages of zircons in drainages containing the peridotite bodies concur with the Re–Os and Sm–Nd data in suggesting that the peridotites were generated by extreme partial melting at least 3 Gyr ago, and subjected to metasomatic refertilization by 2·8–2·9 Ga, and probably in later events as well. A few grains may record even older events, back to *c.* 4·2 Ga. The discordia patterns of the U–Pb data from the zircons with Archean T_{DM} (Fig. 7a) suggest at least three periods of Pb loss, corresponding to the Gothian, Sveconorwegian and Scandian events recorded by crustal zircons from both Greenland and the WGR.

This similarity in post-Archean thermal history does not necessarily imply that the peridotites have resided in the crust since Gothian time. Re–Os data on sulfides in peridotite xenoliths from cratonic areas show model-age peaks that correspond to events in the overlying crust, suggesting that heat and fluids passed through the lithospheric mantle during these major crustal events. Several studies (Zheng *et al.*, 2006*a*, 2006*b*, 2008, in preparation) have shown that U–Pb age data on zircons in peridotitic rocks from the lithospheric mantle mirror age spectra in the overlying crust.

If the peridotite massifs represent the lithospheric mantle beneath the Baltica plate, thrust up into the crust during compressional orogeny, we would expect the existence of some overlying Archean lower crust, and we would expect some Archean contribution to the genesis of the widespread Gothian basement gneisses, and/or to Sveconorwegian-age magmas associated with high-T metamorphism. The zircon data presented in this study show no sign of this contribution. Without convincing evidence for the presence of Archean crust in the WGR, we conclude that the mantle-derived peridotites and the juvenile crust in this part of the Baltic Shield are not genetically related.

The most obvious alternative origin for the peridotites is as fragments of the Laurentian mantle, emplaced in the Baltica crust as it was subducted beneath the North American (Laurentian) plate in Scandian time [the 'sinking emplacement' model of Brueckner (1998)]. Bizzarro *et al.* (2002) used *in situ* U–Pb and Hf-isotope analyses of zircons in ancient (3·0 Ga) carbonatites and kimberlites to argue for an ancient depletion–enrichment cycle in the subcontinental lithospheric mantle beneath SW Greenland. They related the enrichment to carbonatite-style metasomatism, and derived a T_{DM} of 3·4 Ga for this metasomatism; this is essentially similar in style and timing to the metasomatic events inferred from the Almklovdalen data presented here and by Beyer *et al.* (2004).

The Pb-loss pattern in the peridotite-related zircons appears to suggest a thermal history similar to that of the Baltic crust; however, the same sequence of Gothian and Grenvillian events occurred in the crust of East Greenland (Rex & Gledhill, 1981; Kalsbeek *et al.*, 2000; Thrane, 2002; Leslie & Nutman, 2003; Higgins *et al.*, 2004). In addition, the ultradepleted character of the peridotite bodies in Almklovdalen and elsewhere in the WGR is mirrored in the peridotitic xenoliths found in West Greenland basalts (Bernstein *et al.*, 1998, 2006); these rocks also give Re–Os model ages ≥2·9 Ga (Hanghøj *et al.*, 2001), similar to those derived for the WGR peridotites (Beyer *et al.*, 2004).

CONCLUSIONS

The gneisses that make up the crust of the Western Gneiss area were originally generated during the 1·7–1·5 Ga Gothian orogeny. The Hf-isotope signatures of their zircons are juvenile; there is no evidence, from either inherited zircons or the Hf-isotope data, that Archean crustal materials were involved in the genesis of the gneisses.

The Grenville–Sveconorwegian event that overprinted the Gothian gneisses involved an early stage (1·3–1·1 Ga) with significant juvenile additions to the crust, and a later stage (1·1 to <1·0 Ga) in which magmatic rocks were derived largely by remelting of the Gothian basement. Magmas derived during the Sveconorwegian event also show no evidence of Archean contributions.

Zircons with unusual trace-element chemistry, collected from drainages containing mantle-derived peridotite bodies, have Archean U–Pb and Archean Hf model ages; some have had their U–Pb ages partially reset during the Proterozoic and Caledonian thermal events. We interpret these zircons as being derived from the ultramafic bodies, and that they date an Archean refertilization event in the mantle. The absence of any evidence for Archean crust (and hence Archean mantle) beneath southern Baltica leads us to infer that the peridotite massifs represent fragments of the subcontinental lithosphere beneath Laurentia, introduced tectonically into the gneisses during the Caledonian subduction of Baltica beneath the North American plate.

ACKNOWLEDGEMENT

We are grateful to Shelley Allchurch and Felix Genske for help with the analytical work, to Norm Pearson for his continual help and support, and to Jianping Zheng for supplying us with his trace-element data on zircons from the Sulu UHP peridotite massifs in advance of publication. We extend a special thank-you to Sally-Ann Hodgekiss for drafting of the figures, her effort is greatly appreciated. This study used instrumentation funded by ARC LIEF and DEST Systemic Infrastructure Grants, Macquarie University and Industry. The original paper was improved

by thoughtful reviews from Bernard Bingen and Antonio Simonetti, and other comments from an anonymous referee. This is contribution 38 from the ARC Centre of Excellence for Core to Crust Fluid Systems (http://www.ccfs.mq.edu.au) and 804 in the GEMOC Key Centre (http://www.gemoc.mq.edu.au), and contribution 7532 of Lamont–Doherty Earth Observatory of Columbia University.

FUNDING

This work was supported by the Australian Research Council (grant numbers LP0776637, DP0770929) to S.Y.O'R. and W.L.G., and by the National Science Foundation (grant numbers 67663-00 36, 68556-00 37) to H.K.B.

SUPPLEMENTARY DATA

Supplementary data for this paper are available at *Journal of Petrology* online.

REFERENCES

Amelin, Y., Lee, D. C. & Halliday, A. N. (2000). Early–middle Archaean crustal evolution deduced from Lu–Hf and U–Pb isotopic studies of single zircon grains. *Geochimica et Cosmochimica Acta* **64**, 4205–4225.

Andersen, T. (2002). Correction of common Pb in U–Pb analyses that do not report ^{204}Pb. *Chemical Geology* **192**, 59–79.

Andersen, T. B., Jamtveit, B., Dewey, J. F. & Swensson, E. (1991). Subduction and eduction of continental crust: major mechanisms during continent–continent collision and orogenic extensional collapse, a model based on the southern Norwegian Caledonides. *Terra Nova* **3**, 303–310.

Andersen, T., Andresen, A. & Sylvester, B. (2001). Nature and distribution of deep crustal reservoirs in the southwestern part of the Baltic Shield: Evidence from Nd, Sr and Pb isotope data on late Sveconorwegian granites. *Journal of the Geological Society, London* **158**, 253–267.

Andersson, J., Möller, C. & Johansson, L. (2002). Zircon geochronology of migmatite gneisses along the Mylonite Zone (S Sweden): a major Sveconorwegian terrane boundary in the Baltic Shield. *Precambrian Research* **114**, 121–147.

Austrheim, H., Corfu, F., Bryhni, I. & Andersen, T. B. (2003). The Proterozoic Hustad igneous complex: a low strain enclave with a key to the history of the Western Gneiss Region of Norway. *Precambrian Research* **120**, 149–175.

Belousova, E. A., Griffin, W. L., O'Reilly, S. Y. & Fisher, N. I. (2002). Igneous zircon: trace element composition as an indicator of host-rock type. *Contributions to Mineralogy and Petrology* **143**, 602–622.

Belousova, E. A., Reid, A. J., Griffin, W. L. & O'Reilly, S. Y. (2009). Rejuvenation vs recycling of Archean crust in the Gawler Craton, South Australia: Evidence from U–Pb and Hf isotopes in detrital zircon. *Lithos* **113**, 570–582.

Belousova, E. A., Kostitsyn, Y. A., Griffin, W. L., Begg, G. C., O'Reilly, S. Y. & Pearson, N. J. (2010). The growth of the continental crust: Constraints from zircon Hf-isotope data. *Lithos* **119**, 457–466.

Bernstein, S., Kelemen, P. B. & Brooks, C. K. (1998). Highly depleted spinel harzburgite xenoliths in Tertiary dikes from East Greenland. *Earth and Planetary Science Letters* **154**, 221–235.

Bernstein, S., Hanghøj, K., Kelemen, P. B. & Brooks, C. K. (2006). Ultra-depleted shallow cratonic mantle beneath West Greenland: dunitic xenoliths from Ubekendt Ejland. *Contributions to Mineralogy and Petrology* **152**, 335–347.

Beyer, E. E., Brueckner, H. K., Griffin, W. L., O'Reilly, S. Y. & Graham, S. (2004). Archean mantle fragments in Proterozoic crust, Western Gneiss Region, Norway. *Geology* **32**, 609–612.

Beyer, E. E., Griffin, W. L. & O'Reilly, S. Y. (2006). Transformation of Archaean lithospheric mantle by refertilization: evidence from exposed peridotites in the Western Gneiss Region, Norway. *Journal of Petrology* **47**, 1611–1636.

Bingen, B., Andersson, J., Söderlund, U. & Möller, C. (2008). The Mesoproterozoic in the Nordic countries. *Episodes* **31**, 1–6.

Bizzarro, M., Simonetti, A., Stevenson, R. K. & David, J. (2002). Hf isotope evidence for a hidden mantle reservoir. *Geology* **30**, 771–774.

Brueckner, H. K. (1972). Interpretation of Rb–Sr ages from the Precambrian and Paleozoic rocks of southern Norway. *American Journal of Science* **272**, 334–358.

Brueckner, H. K. (1979). Precambrian ages from the Geiranger–Tafjord–Grotli area of the basal gneiss region, southwestern Norway. *Norsk Geologiske Tidsskrift* **59**, 141–153.

Brueckner, H. K. (1998). Sinking intrusion model for the emplacement of garnet-bearing peridotites into continent collision orogens. *Geology* **26**, 631–634.

Brueckner, H. K. (2006). Dunk, dunkless and re-dunk tectonics: a model for metamorphism, lack of metamorphism, and repeated metamorphism of HP/UHP terranes. *International Geological Review* **48**, 978–995.

Brueckner, H. K. (2009). Subduction of continental crust, the origin of post-orogenic granitoids (and anorthosites?) and the evolution of Fennoscandia. *Journal of the Geological Society, London* **166**, 753–762.

Brueckner, H. K., Blusztajn, J. & Bakun-Czubarow, A. (1996). Trace element and Sm–Nd 'age' zoning in garnets from peridotites of the Caledonian and Variscan Mountains and tectonic implications. *Journal of Metamorphic Geology* **14**, 61–73.

Brueckner, H. K., Carswell, D. A. & Griffin, W. L. (2002). Paleozoic diamonds within a Precambrian peridotite lens in UHP gneisses of the Norwegian Caledonides. *Earth and Planetary Science Letters* **203(3–4)**, 805–816.

Brueckner, H. K. & Van Roermund, H. L. M. (2004). Dunk Tectonics: a multiple subduction/eduction model for the evolution of the Scandinavian Caledonides. *Tectonics* **23**, TC2004, doi:10.1029/2003TC001502.

Brueckner, H. K., Carswell, D. A., Griffin, W. L., Medaris, L. G., Jr, Van Roermund, H. L. M. & Cuthbert, S. J. (2010). The mantle and crustal evolution of two garnet peridotite suites from the Western Gneiss Region, Norwegian Caledonides: an isotopic investigation. *Lithos* **117**, 1–19.

Bryhni, I. & Grimstad, E. (1970). Supracrustal and infracrustal rocks in the Gneiss Region of the Caledonides west of Breimsvatn. *Norges Geologisk Undersøkelse* **266**, 105–150.

Carswell, D. A. (1986). The metamorphic evolution of Mg–Cr type Norwegian garnet peridotites. *Lithos* **19**, 279–297.

Carswell, D. A., Brueckner, H. K., Cuthbert, S. J., Mehta, K. & O'Brien, P. J. (2003*a*). The timing of stabilisation and exhumation rate for ultra-high pressure rocks in the Western Gneiss Region of Norway. *Journal of Metamorphic Geology* **21**, 602–612.

Carswell, D. A., Tucker, R. R., O'Brien, P. J. & Krogh, T. E. (2003*b*). Coesite micro-inclusions and the U/Pb age of zircons from the

Hareidland Eclogite in the Western Gneiss Region of Norway. *Lithos* **67**, 181–190.

Cuthbert, S. J., Harvey, M. A. & Carswell, D. A. (1983). A tectonic model for the metamorphic evolution of the Basal Gneiss Complex, western south Norway. *Journal of Metamorphic Geology* **1**, 63–90.

Cuthbert, S. J., Carswell, D. A., Krogh-Ravna, E. J. & Wain, A. (2000). Eclogites and eclogites in the Western Gneiss Region, Norwegian Caledonides. *Lithos* **52**, 165–195.

Eskola, P. (1921). On the eclogites of Norway. *Det Norske Videnskapsselskapet i Kristiania, I Matematisk-Naturvideskapelig Klasse* **8**, 1–118.

Gebauer, D., Lappin, M. A., Grunenfelder, M. & Wyttenbach, A. (1985). The age and origin of some Norwegian eclogites—U–Pb zircon and REE study. *Chemical Geology* **52**, 227–247.

Griffin, W. L. & Brueckner, H. K. (1980). Caledonian Sm–Nd ages and a crustal origin for Norwegian eclogites. *Nature* **285**, 319–321.

Griffin, W. L. & Brueckner, H. K. (1985). REE, Rb–Sr and Sm–Nd studies of Norwegian eclogites. *Chemical Geology* **52**, 249–271.

Griffin, W. L. & Qvale, H. (1985). Superferrian eclogites and the crustal origin of garnet peridotites: Almklovdalen, Norway. In: Gee, D. G. & Sturt, B. A. (eds) *The Caledonide Orogen—Scandinavia and Related Areas*. Chichester: John Wiley, pp. 803–812.

Griffin, W. L., Pearson, N. J., Belousova, E., Jackson, S. E., O'Reilly, S. Y., van Achterberg, E. & Shee, S. R. (2000). The Hf isotope composition of cratonic mantle: LAM-MC-ICPMS analysis of zircon megacrysts in kimberlites. *Geochimica et Cosmochimica Acta* **64**, 133–147.

Griffin, W. L., Wang, X., Jackson, S. E., Pearson, N. J., O'Reilly, S. Y., Xu, X. & Zhou, X. (2002). Zircon chemistry and magma mixing, SE China: *In-situ* analysis of Hf isotopes, Pingtan and Tonglu igneous complexes. *Lithos* **61**, 237–269.

Griffin, W. L., Pearson, N. J., Belousova, E. A. & Saeed, A. (2007). Reply to 'Comment to short-communication 'Comment: Hf-isotope heterogeneity in zircon 91500' by W. L. Griffin, N. J. Pearson, E. A. Belousova and A. Saeed (Chemical Geology 233 (2006) 358–363)' by F. Corfu. *Chemical Geology* **244**, 354–356.

Griffin, W. L., Powell, W. J., Pearson, N. J. & O'Reilly, S. Y. (2008). GLITTER: data reduction software for laser ablation ICP-MS. In: Sylvester, P. (ed.) . *Laser Ablation–ICP–MS in the Earth Sciences. Mineralogical Association of Canada, Short Course Series* **40(Appendix 2)**, 204–207.

Hacker, B. R., Andersen, T. B., Johnston, S., Kylander-Clark, A. R. C., Peterman, E. M., Walsh, E. O. & Young, D. (2010). High-temperature deformation during continental-margin subduction & exhumation: The ultrahigh-pressure Western Gneiss Region of Norway. *Tectonophysics* **480(1–4)**, 149–171, doi:101016/j.tecto.2009.08.012.

Hanghøj, K., Kelemen, P., Bernstein, S., Blusztajn, J. & Frei, R. (2001). Os isotopes in the Weidemann Fjord mantle xenoliths: a unique record of cratonic mantle formation by melt depletion in the Archean. *Geochemistry, Geophysics, Geosystems* **2**, paper no. 2000GC000085.

Harley, S. L. & Carswell, D. A. (1995). Ultradeep crustal metamorphism: A prospective view. *Journal of Geophysical Research* **100**, 8367–8380.

Higgins, A. K., Elvevold, S., Escher, J. C., Frederiksen, K. S., Gilotti, J. A., Henriksen, N., Jepsen, H. F., Jones, K. A., Kalsbeek, F., Kinny, P. D., Leslie, A. G., Smith, M. P., Thrane, K. & Watt, G. R. (2004). The foreland-propagating thrust architecture of the East Greenland Caledonides, 72°–75°N. *Journal of the Geological Society, London* **161**, 1009–1026.

Jackson, S. E., Pearson, N. J., Griffin, W. L. & Belousova, E. A. (2004). The application of laser ablation-inductively coupled plasma-mass spectrometry to *in-situ* U–Pb zircon geochronology. *Chemical Geology* **211**, 47–69.

Jamtveit, B., Carswell, D. A. & Mearns, E. W. (1991). Chronology of the high-pressure metamorphism of Norwegian garnet peridotites/pyroxenites. *Journal of Metamorphic Geology* **9**, 125–139.

Kalsbeek, F., Thrane, K., Nutman, A. P. & Jepsen, H. F. (2000). Late Mesoproterozoic to early Neoproterozoic history of the East Greenland Caledonides: evidence for Grenvillian orogenesis? *Journal of the Geological Society, London* **157**, 1215–1225.

Krogh, E. J. (1977). Evidence for a Precambrian continent–continent collision in western Norway. *Nature* **267**, 17–19.

Krogh, T., Robinson, P. & Terry, M. P. (2003). Precise U–Pb zircon ages define 18 and 19 m.y. subduction to uplift intervals in the Averøya–Nordøyane area, Western Gneiss Region. In: Eide, E. A. (ed.) . *The Alice Wain Memorial West Norway Eclogite Field Symposium, Abstract Volume. Norges Geologiske Undersøkelse Report* **2003.055**, 71–72.

Kylander-Clark, A. R. C., Hacker, B. R., Johnson, C. M., Beard, B. L., Mahlen, J. J. & Lapen, T. J. (2007). Coupled Lu–Hf and Sm–Nd geochronology constrains prograde and exhumation histories of high- and ultrahigh-pressure eclogites from western Norway. *Chemical Geology* **242**, 137–154.

Kylander-Clark, A. R. C., Hacker, B. R. & Mattinson, J. M. (2008). Slow exhumation of UHP terranes: titanite and rutile ages of the Western Gneiss Region. *Earth and Planetary Science Letters* **272**, 531–540.

Lapen, T. J., Medaris, L. G., Jr, Johnson, C. M. & Beard, B. L. (2005). Archean to Middle Proterozoic evolution of Baltica subcontinental lithosphere: Evidence from combined Sm–Nd and Lu–Hf isotope analyses of the Sandvik ultramafic body, Norway. *Contributions to Mineralogy and Petrology* **150**, 131–145.

Lapen, T. J., Medaris, L. G., Jr, Beard, B. L. & Johnson, C. M. (2009). The Sandvik peridotite, Gurskøy, Norway: Three billion years of mantle evolution in the Baltica lithosphere. *Lithos* **109**, 145–154.

Lauri, L. S., Andersen, T., Hölttä, P., Huhma, H. & Graham, S. (2011). Evolution of the Archaean Karelian Province in the Fennoscandian Shield in the light of U–Pb zircon ages and Sm–Nd and Lu–Hf isotope systematics. *Journal of the Geological Society, London* **168**, 201–218.

Leslie, A. G. & Nutman, A. P. (2003). Evidence for Neoproterozoic orogenesis and early high temperature Scandian deformation events in the southern East Greenland Caledonides. *Geological Magazine* **140**, 309–333.

Mearns, E. W. (1986). Sm–Nd ages for Norwegian garnet peridotite. *Lithos* **19**, 269–278.

Mearns, E. W. & Lappin, M. A. (1982). A Sm–Nd isotopic study of 'internal' and 'external' eclogites, garnet lherzolite and grey gneiss from Almklovdalen, western Norway. *Terra Cognita* **2**, 324.

Medaris, L. G., Jr (1980). Petrogenesis of the Lien peridotite and associated eclogites, Almklovdalen, western Norway. *Lithos* **13**, 339–353.

Medaris, L. G., Jr (1984). A geothermobarometric investigation of garnet peridotites in the Western Gneiss Region of Norway. *Contributions to Mineralogy and Petrology* **87**, 72–86.

Medaris, L. G., Jr & Carswell, D. A. (1990). Petrogenesis of Mg–Cr garnet peridotites in European metamorphic belts. In: Carswell, D. A. (ed.) *Eclogite Facies Rocks*. Glasgow: Blackie, pp. 260–290.

Mørk, M. B. E. & Mearns, E. W. (1986). Sm–Nd isotopic systematics of a gabbro–eclogite transition. *Lithos* **19**, 255–267.

Osland, R. (1997). Modelling of variations in Norwegian olivine deposits. Doktor Ingeniør Thesis, Norwegian University of Science and Technology, Trondheim, 189 pp.

Peterman, E. M., Hacker, B. R. & Baxter, E. F. (2009). Phase transformations of continental crust during subduction and exhumation: Western Gneiss Region, Norway. *European Journal of Mineralogy* **21**, 1097–1118.

Rex, D. C. & Gledhill, A. R. (1981). Isotopic studies in the East Greenland Caledonides 72°–74°N—Precambrian and Caledonian ages. *Rapport Grønlands Geologiske Undersøgelse* **104**, 47–72.

Roberts, D. (2003). The Scandinavian Caledonides: event chronology, paleogeographic settings and likely modern analogues. *Tectonophysics* **365**, 283–299.

Roberts, D. & Gee, D. G. (1985). An introduction to the structure of the Scandinavian Caledonides. In: Gee, D. G. & Sturt, B. A. (eds) *The Caledonide Orogen—Scandinavia and Related Areas*. Chichester: John Wiley, pp. 55–68.

Root, D. B., Hacker, B. R., Mattinson, J. M. & Wooden, J. L. (2004). Zircon geochronology and ca 400 Ma exhumation of Norwegian ultrahigh-pressure rocks: an ion microprobe and chemical abrasion study. *Earth and Planetary Science Letters* **228**, 325–341.

Root, D. B., Hacker, B. R., Gans, P. B., Ducea, M. N., Eide, E. A. & Mosenfelder, L. (2005). Discrete ultrahigh-pressure domains in the Western Gneiss Region, Norway: implications for formation and exhumation. *Journal of Metamorphic Geology* **23**, 45–61.

Scherer, E., Münker, C. & Mezger, K. (2001). Calibration of the lutetium–hafnium clock. *Science* **293**, 683–687.

Schmidberger, S. S., Heaman, L. M., Simonetti, A., Creaser, R. A. & Cookenboo, H. O. (2005). Formation of Paleoproterozoic eclogitic mantle, Slave Province (Canada): Insights from *in-situ* Hf and U–Pb isotopic analyses of mantle zircons. *Earth and Planetary Science Letters* **240**, 621–633.

Skår, O. & Pedersen, R. B. (2003). Relations between granitoid magmatism and migmatization: U–Pb geochronological evidence from the Western Gneiss Complex, Norway. *Journal of the Geological Society, London* **160**, 935–946.

Spengler, D., van Roermund, H. L. M., Drury, M. R., Ottolini, L., Mason, R. D. & Davies, G. R. (2006). Deep origin and hot melting of an Archaean orogenic peridotite massif in Norway. *Nature* **440**, 913–917.

Spengler, D., Brueckner, H. K., van Roermund, H. L. M., Drury, M. R. & Mason, P. R. D. (2009). Long-lived, cold burial of Baltica towards 200 km depth. *Earth and Planetary Science Letters* **281**, 27–35.

Stephens, M. B. & Gee, D. G. (1989). Terranes and polyphase accretionary history in the Scandinavian Caledonides. In: Dallmeyer, R.D. (ed) *Terranes in the circum-Altalntic Paleozoic orogens. Geological Society of America, Special Papers* **230**, 17–30.

Thrane, K. (2002). Relationships between Archaean and Palaeoproterozoic crystalline basement complexes in the southern part of the East Greenland Caledonides: an ion microprobe study. *Precambrian Research* **113**, 19–42.

Tucker, R. D., Råheim, A., Krogh, T. E. & Corfu, F. (1987). Uranium–lead zircon and titanite ages from the northern portion of the Western Gneiss Region, south–central Norway. *Earth and Planetary Science Letters* **81**, 203–211.

Tucker, R. D., Krogh, T. E. & Råheim, A. (1990). Proterozoic evolution and age-province boundaries in the central part of the Western Gneiss Region, Norway: Results of U–Pb dating of accessory minerals from Trondheimsfjord to Geiranger. In: Gower, C. F., Ryan, B. & Rivers, T. (eds) *Middle Proterozoic Geology of the Southern Margin of Proto Laurentia–Baltica. Geological Association of Canada, Special Papers* **38**, 149–173.

Tucker, R. D., Robinson, P., Solli, A., Gee, D. G., Thorsnes, T., Krogh, T. E., Nordgulen, Ø. & Bickford, M. E. (2004). Thrusting and extension in the Scandian Hinterland, Norway: New U–Pb ages and tectonostratigraphic evidence. *American Journal of Science* **304**, 477–532.

Waldron, J. W. F., Floyd, J. D., Simonetti, A. & Heaman, L. M. (2008). Ancient Laurentian detrital zircon in the closing Iapetus Ocean, Southern Uplands terrane, Scotland. *Geology* **36**, 527–530.

Walsh, E. O. & Hacker, B. R. (2004). The fate of subducted continental margins: two-stage exhumation of the high-pressure to ultrahigh-pressure Western Gneiss Complex, Norway. *Journal of Metamorphic Geology* **22**, 671–689.

Walsh, E. O., Hacker, B. R., Gans, P. B., Grove, M. & Gehrels, G. (2007). Protolith ages and exhumation histories of (ultra) high-pressure rocks across the Western Gneiss Region. *Geological Society of America Bulletin* **119**, 289–301.

Young, D. J., Hacker, B. R., Andersen, T. B. & Corfu, F. (2007). Prograde amphibolite facies to ultrahigh-pressure transition along Nordfjord, western Norway: Implications for exhumation tectonics. *Tectonics* **26**, 1–15.

Zhang, R. Y., Li, T., Rumble, D., Yui, T.-F., Li, L., Yang, J. S., Pan, Y. & Liou, J. G. (2007). Multiple metasomatism in Sulu ultrahigh-*P* garnet peridotite constrained by petrological and geochemical investigations. *Journal of Metamorphic Geology* **25**, 149–164.

Zhang, R. Y., Liou, J. G., Zheng, J. P., Griffin, W. L., Yang, Y.-H. & Jahn, B.-M. (2009). Petrogenesis of eclogites enclosed in mantle-derived peridotites from the Sulu UHP terrane: constraints from trace elements in minerals and Hf isotopes in zircon. *Lithos* **109**, 176–192.

Zheng, J., Griffin, W. L., O'Reilly, S. Y., Zhang, M. & Pearson, N. (2006*a*). Zircons in mantle xenoliths record the Triassic Yangtze–North China continental collision. *Earth and Planetary Sciences* **247**, 130–142.

Zheng, J. P., Griffin, W. L., O'Reilly, S. Y., Yang, J. S. & Zhang, R. Y. (2006*b*). A refractory mantle protolith in younger continental crust, east–central China: Age and composition of zircon in the Sulu UHP peridotite. *Geology* **34**, 705–708.

Zheng, J. P., Griffin, W. L., O'Reilly, S. Y., Hu, B. Q., Zhang, M., Pearson, N. J., Lu, F. X. & Wang, F. Z. (2008). Continental collision and accretion recorded in the deep lithosphere of central China. *Earth and Planetary Science Letters* **269**, 496–506.